Digital Comprehensive Summaries of Uppsala Dissertations
from the Faculty of Medicine 1962

Harnessing the molecular Trojan horse

Evaluating properties of preclinical Aβ immunoPET radioligands for optimized brain delivery via the transferrin receptor

GILLIAN BONVICINI

ACTA UNIVERSITATIS
UPSALIENSIS
2023

ISSN 1651-6206
ISBN 978-91-513-1857-8
urn:nbn:se:uu:diva-507816

UPPSALA
UNIVERSITET

Dissertation presented at Uppsala University to be publicly examined in Rudbecksalen, Rudbecklaboratoriet, Dag Hammarskjölds väg 20, Uppsala, Thursday, 21 September 2023 at 09:15 for the degree of Doctor of Philosophy (Faculty of Medicine). The examination will be conducted in English. Faculty examiner: PhD Joy Zuchero (Denali Therapeutics Inc.).

Abstract
Bonvicini, G. 2023. Harnessing the molecular Trojan horse. Evaluating properties of preclinical Aβ immunoPET radioligands for optimized brain delivery via the transferrin receptor. *Digital Comprehensive Summaries of Uppsala Dissertations from the Faculty of Medicine* 1962. 62 pp. Uppsala: Acta Universitatis Upsaliensis. ISBN 978-91-513-1857-8.

With high specificity and selectivity to targets, antibodies are prime candidates for positron emission tomography (PET) radioligands. They do not passively cross the blood-brain barrier which has hindered their development for imaging intrabrain targets, like amyloid-β (Aβ) in Alzheimer's disease. The molecular Trojan horse strategy with antibodies that bind to both the transferrin receptor (TfR) and an intrabrain target improves brain delivery of therapeutic antibodies. However, therapeutic antibodies are typically dosed substantially higher than antibody-based PET (immunoPET) radioligands.

This thesis evaluated the effects of affinity, valency, and dose on the brain delivery of preclinical Aβ immunoPET radioligands via the TfR.

Paper I investigated whether immunoPET with TfR-mediated brain delivery could image Aβ with similar sensitivity in rats as it has in mice. To our knowledge, this was the first time TfR-hijacking to deliver a radioligand to image Aβ was successfully demonstrated in rats; suggesting this strategy could eventually be translated to clinics.

Affinity to TfR influences therapeutic delivery to the brain. In Paper II, we compared four Biacore setups and one on-cell assay for determining apparent affinities to the TfR. Absolute affinity determination was challenging since several assay conditions impacted the kinetic parameters. A directional TfR capture in Biacore may be optimal since it determined kinetic parameters while mimicking *in vivo* receptor conditions. Papers I and III investigated how antibody affinity affects brain delivery at tracer doses and indicated that stronger TfR affinity yielded higher brain delivery. The antibodies in Paper III lacked effector function. The resulting pharmacokinetic profiles in Aβ pathology-presenting mice indicated this may have improved target accumulation of the immunoPET radioligand.

In Paper IV, we screened a novel library of monovalent and bivalent affinity variants of the anti-mouse TfR antibody, 8D3. A pair of monovalent and bivalent antibodies with an apparent affinity of 10 nM was identified and evaluated *in vivo*. Monovalent binding yielded higher brain uptake at a tracer dose but whether bivalent binding steered the antibody towards lysosomal degradation was unclear.

In conclusion, monovalency, high affinity binding, and ablated effector function are likely beneficial properties for TfR-mediated brain delivery of an immunoPET radioligand at a tracer dose.

Keywords: Transferrin receptor (TfR), bispecific antibody, brain delivery, positron emission tomography (PET), Alzheimer's disease, pharmacokinetics

Gillian Bonvicini, Department of Public Health and Caring Sciences, Geriatrics, Box 609, Uppsala University, SE-75125 Uppsala, Sweden.

ISSN 1651-6206
ISBN 978-91-513-1857-8
URN urn:nbn:se:uu:diva-507816 (http://urn.kb.se/resolve?urn=urn:nbn:se:uu:diva-507816)

"Isn't it splendid to think of all the things that there are to find out about?
It's such an interesting world.
It wouldn't be half so interesting if we know all about everything, would it?"

– Anne of Green Gables
(L.M. Montgomery)

List of Papers

This thesis is based on the following papers, which are referred to in the text by their Roman numerals.

I. **Bonvicini, G.**, Syvänen, S., Andersson, K.G., Haaparanta-Solin, M., López-Picón, F., Sehlin, D. (2022) ImmunoPET imaging of amyloid-beta in a rat model of Alzheimer's disease with a bispecific, brain-penetrating fusion protein. *Translational Neurodegeneration*, 11(55):1–14.

II. **Bonvicini, G.**, Singh, S., Nygren, P., Xiong, M., Syvänen, S., Sehlin, D., Falk, R., Andersson, K.G. Comparing *in vitro* affinity measurements of antibodies to TfR1: surface plasmon resonance versus on-cell affinity. *Submitted.*

III. **Bonvicini, G.**, Singh, S., Sandersjöö, L., Dallas, T., Schlein, E., Sehlin, D., Andersson, K.G., Syvänen, S. Stronger affinity to Transferrin receptor enhances detection of amyloid-β pathology with bispecific antibody radioligands at a tracer dose. *Manuscript.*

IV. **Bonvicini, G.**, Singh, S., Sandersjöö, L., Sehlin, D., Syvänen, S., Andersson, K.G. Evaluation of valency effects on TfR-mediated brain delivery *in vivo*. *Manuscript.*

Additional Publications

Publications not included as part of this thesis:

I. Faresjö, R., **Bonvicini, G.**, Fang, X.T., Sehlin, D., Syvänen, S. (2021) Brain pharmacokinetics of two BBB penetrating bispecific antibodies of different sizes. *Fluids Barriers CNS*, 18(1):26.

II. Syvänen, S., Meier S.R., Roshanbin, S. Xiong, M., Faresjö, R., Gustavsson, T., **Bonvicini, G.**, Schlein, E., Aquilar, X., Julku, U., Eriksson, J., Sehlin, D. (2022) PET imaging in preclinical anti-Aβ drug development. *Pharmaceutical Research*, 39(7):1481-1496.

Contents

Abbreviations

γ	gamma photon
[^{11}C]PiB	[^{11}C]Pittsburgh Compound-B
^{18}F	fluorine-18
[^{18}F]FDG	[^{18}F]fluorodeoxyglucose
^{124}I	iodine-124
^{125}I	iodine-125
Aβ	Amyloid-beta
AD	Alzheimer's disease
ADCC	Antibody-dependent cellular cytotoxicity
ADCP	Antibody-dependent cellular phagocytosis
ApoE	Apolipoprotein E
APP	Amyloid precursor protein
ATP	Adenosine triphosphate
Bapi	Bapineuzumab
BBB	Blood-brain barrier
C1q	Complement protein 1q
CDC	Complement-dependent cytotoxicity
CNS	Central nervous system
e^-	electron
e^+	positron
ELISA	Enzyme-linked immunosorbent assay
Fab	Fragment antigen binding
Fc	Fragment crystallisable
FcγR	Fc-gamma receptor
FDA	Food and Drug Administration
H-Ft	Heavy-chain ferritin
IDS	Iduronate-2-sufatase
KiH	Knob-into-hole
MCI	Mild cognitive impairment
PET	Positron emission tomography
PSEN1	Presenilin-1
PSEN2	Presenilin-2
SPECT	Single-photon emission computed tomography
SPR	Surface plasmon resonance
TCO	Trans-cyclooctene
Tf	Transferrin

TfR	Transferrin receptor
UniProt	Universal Protein Resource
WT	Wild-type

Introduction

Alzheimer's disease

Dementia is an umbrella term for conditions that affect memory and cognitive function and is the seventh leading cause of death in the world today. The most common form, accounting for approximately 60-70% of all dementia cases, is Alzheimer's disease (AD)[1]. It is a neurodegenerative disease characterized by worsening memory loss and decline in cognitive function[2].

Alois Alzheimer first described AD in 1906[3]. He had a patient, Auguste Deter, who presented with memory impairment and other cognitive symptoms. After her death, Alzheimer found cortical thinning, senile plaques, and neurofibrillary tangles during an autopsy of her brain[3]. Nearly 120 years later, these plaques and neurofibrillary tangles are still considered the two main neuropathological hallmarks of AD. Both are composed of aggregated proteins: the extracellular plaques are deposits of aggregated amyloid-beta (Aβ)[4,5] while the neurofibrillary tangles are composed of hyperphosphorylated tau[6,7].

As a progressive disease, AD has many stages with the pathophysiological changes starting around 20 years before clinical symptoms emerge[8]. This is known as the preclinical stage. Clinical symptoms will slowly begin to appear during the mild cognitive impairment (MCI) stage and worsen as the patient progresses to the severe stages of AD. Advances in diagnostic tools, including fluid biomarkers (plasma and cerebrospinal fluid) and medical imaging techniques, make it possible to reliably identify and monitor these neuropathological changes years before clinical symptoms appear[2].

There are two types of AD: sporadic AD making up the majority of cases (>95%) and familial AD[9]. Sporadic AD generally affects patients of 65 years or older and therefore, is also called late-onset AD. Risk factors for sporadic AD include age, vascular health, and some genetic risk factors, such as, most notably, polymorphisms in the apolipoprotein E (ApoE) alleles[10]. Familial AD has an early age of onset (i.e. younger than 65 years). It is inherited via mutations in genes involved with Aβ peptide production: amyloid precursor protein (*APP*), presenilin-1 (*PSEN1*) or presenilin-2 (*PSEN2*)[9,11–14].

Amyloid cascade hypothesis

Over the last few decades, a generally accepted theory is that one of the main driving mechanisms for AD is the underlying accumulation and aggregation of pathological Aβ peptides. Cleavage of APP via the amyloidogenic pathway produces soluble Aβ peptides ranging from 37 to 43 amino acids long. $Aβ_{1-40}$ and $Aβ_{1-42}$ are the most common isoforms[13]. Soluble Aβ monomers are thought to have multiple physiological functions, including modulating neurogenesis, synaptogenesis, and angiogenesis; regulating learning and memory; maintaining the blood-brain barrier (BBB); protecting against oxidative stress; and acting as an antimicrobial peptide[15]. In AD, misfolded Aβ monomers bind together to form dimers and trimers (Fig. 1). These small aggregates continue to grow into larger oligomers which further aggregate into the largest soluble form, protofibrils. Aggregates finally deposit into insoluble, β-sheet-rich fibrils and plaques[16].

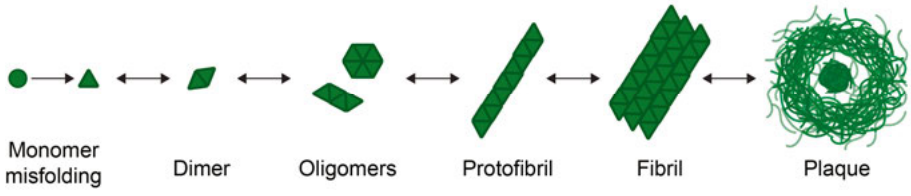

Figure 1. Aβ aggregation pathway.

When Aβ was first hypothesized to be the cause of AD in the amyloid cascade hypothesis, it was proposed that the insoluble plaques were the toxic aggregate species causing neurodegeneration and cognitive decline[17]. However, Aβ plaque loads do not correlate with disease severity and cognitive decline in patients while oligomer levels do[18–20]. Moreover, Aβ oligomers and protofibrils seem to induce neuronal cell death and astrocytic activation *in vitro*[21–24]. Therefore, the amyloid cascade hypothesis has been updated to focus on oligomers and protofibrils as the more toxic forms of aggregated Aβ[25,26].

There is a vast amount of scientific evidence supporting that Aβ aggregates play a causative role in AD pathogenesis. Mutations causing familial AD are in genes involved with Aβ peptide production and the ratio of $Aβ_{1-40}$ and $Aβ_{1-42}$[13]. The introduction of these mutations in animals can also lead to AD pathophysiology and symptoms[27]. Biomarker studies in humans indicate that Aβ aggregation is the first step in AD pathogenesis and is detectable several years before other diagnostic indicators such as tau aggregation, neurodegeneration, or clinical symptoms[28]. Furthermore, Aβ-targeting immunotherapies improve clinical symptoms[29,30]. Aβ aggregation is also considered the trigger for the other pathophysiological mechanisms in AD including hyperphosphorylated tau aggregation, neuroinflammation, oxidative stress, and mitochon-

drial dysfunction[15,25]. Despite the evidence supporting the toxic role of Aβ aggregates, the roles of these other pathophysiological mechanisms should not be overlooked.

Immunotherapies targeting Aβ

Although there are currently no curative treatments available for AD, several disease-modifying, passive immunotherapies have recently completed late-phase clinical trials.

The first AD drug introduced to the market since 2003 was **aducanumab** (marketed as Aduhelm). Developed by Biogen, aducanumab is a human IgG1 monoclonal antibody that binds residues 3-7 of the N-terminus of Aβ[31]. It selectively binds to Aβ aggregates over monomers[31,32]. In July 2021, aducanumab received accelerated approval for treating AD in the USA by the Food and Drug Administration (FDA)[33]. However, this decision was extensively criticized within the field[29,34,35] since the two phase III clinical trials, EMERGE (NCT02484547) and ENGAGE (NCT02477800), were stopped midway due to futility. After revising the separate datasets, Biogen concluded that there was significant improvement in the clinical dementia staging with the Clinical Dementia Rating Sum of Boxes (the primary endpoint) in the EMERGE trial[29]. There was also drug-related reduction in the Aβ plaque load as measured by Aβ positron emission tomography (PET) in both trials[29].

Lecanemab (marketed as Leqembi) was the second monoclonal antibody to be granted accelerated approval by the FDA and the first AD-targeting immunotherapy to have the accelerated approval converted to traditional approval in July 2023[36,37]. It is the humanized IgG1 version of mAb158, an anti-Aβ antibody developed by BioArctic in collaboration with Uppsala University in Sweden. Lecanemab binds preferentially to Aβ oligomers and protofibrils than to fibrils and monomers[38,39]. In the phase III CLARITY AD trial (NCT03887455), lecanemab showed highly significant reduction in clinical decline compared to the placebo after 18 months. All of the secondary endpoints were also statistically significant compared to the placebo[30].

Eli Lilly & Co. has developed another promising humanized IgG1 antibody for treating AD called **donanemab**. It is derived from the murine antibody, mE8-IgG2, and binds to $Aβ_{p3-42}$, an N-terminus truncated, pyroglutamate form of Aβ[40]. $Aβ_{p3-42}$ is found in dense and diffuse amyloid plaques[41]. It is more hydrophobic than $Aβ_{1-42}$ and thus, is thought to play a role in accelerating Aβ aggregation kinetics and plaque seeding[42]. The phase III TRAILBLAZER-ALZ 2 trial (NCT04437511) ended in May 2023 and met the primary endpoint and all secondary endpoints[43]. Overall, donanemab significantly slowed cognitive and functional decline in patients with MCI or mild AD[43].

Gantenerumab is a human IgG1 antibody developed by Hoffman-La Roche that targets the N-terminus and central amino acids of Aβ fibrils[44]. To

date, it was the only antibody being tested with a subcutaneous route of administration in a phase III trial[45]. However, it recently failed to meet its phase III GRADUATE trial's primary endpoint (NCT03444870) of slowing clinical decline in patients with MCI or mild AD. Roche currently has a phase I/II trial (NCT04639050) ongoing with a redesigned version of gantenerumab called **trontinemab**. Trontinemab is gantenerumab linked to Roche's brain shuttle technology to enhance brain delivery via the transferrin receptor (TfR)[46,47]. The phase I/II trial is expected to conclude in 2025.

PET in AD

PET is an imaging technique that allows for the depiction and quantification of physiological and biochemical changes *in vivo*. It has become an important tool during the last couple of decades in both diagnosing AD patients and assessing a therapy's effectiveness[48,49]. The development of [^{18}F]fluorodeoxyglucose ([^{18}F]FDG) in 1979 meant that glucose metabolism could be visualized. There are characteristic changes in glucose consumption in different neurodegenerative diseases that can be identified with [^{18}F]FDG-PET. For example, this PET tracer can differentiate diagnoses between AD and other dementias such as Lewy Body dementia or frontotemporal dementia because AD patients typically display lowered temperoparietal glucose metabolism[50].

With the increased research indicating that Aβ aggregation plays a role in progression, even before symptoms appear, there was a surge in efforts to develop radioligands to track the formation of amyloid plaques. In the early 2000s, the small molecular radioligand, [^{11}C]Pittsburgh Compound-B ([^{11}C]PiB), was the first compound synthesized to visualize Aβ plaques[51]. [^{11}C]PiB and the later-established fluorine-18 (^{18}F)-labelled analogues are still the gold-standard in clinical trials of novel Aβ reducing treatments for AD patient enrolment and tracking plaque development[49,52]. These small molecule radioligands have helped to increase diagnostic confidence of AD[48]. However, they do not detect the toxic, soluble oligomeric and protofibrillar Aβ species[53] nor the diffuse Aβ plaques, such as those found in AD patients with the *Arctic APP* mutation[54]. This is because these radioligands bind to the β-sheet structure in amyloid plaques. Therefore, these radioligands also have difficulties discriminating between different proteins with similar fibrillary structures, such as aggregated Aβ and alpha-synuclein[52]. Although Aβ and tau aggregates are the predominant pathologies in AD, patients frequently exhibit co-pathologies of additional proteinopathies common in other neurodegenerative diseases[55,56] which can lead to incorrect diagnoses.

With the shift in the AD field for therapeutic biologics that primarily target smaller Aβ aggregates, it would be beneficial to have diagnostics that detect these aggregate species as well. Better matched diagnostic tools to the pathological targets of the emerging immunotherapeutics will aid in the selection of

patients for clinical trials, the evaluation of therapeutic effect during the trial, and the monitoring of patients receiving the treatment once approved. Thus, antibody and antibody fragment-based radioligands against Aβ are being developed. Antibodies have high specificity and selectivity to targets and their use as PET tracers have become quite common for peripheral PET in oncology during the last decades[57–59]. One main limitation explaining why they are not currently used for central nervous system (CNS) PET is that they do not cross the BBB well. At 150 kDa, antibodies are large, lipophobic molecules. Less than 0.05% of the injected antibody dose passes into the brain after intravenous injection[60–63]. This makes it difficult to reach sufficient levels of antibody in the brain to achieve an adequate signal-to-noise ratio for *in vivo* imaging.

Blood-brain barrier (BBB)

The BBB is a biological barrier that prevents direct access from the circulatory system to the brain parenchyma. It plays a critical role in CNS protection and maintaining homeostasis. Therefore, the BBB poses a significant obstacle for delivering therapeutic and diagnostic compounds to the brain and is the focus of countless thorough reviews[64–68]. The BBB is part of the neurovascular unit which consists of brain capillary endothelial cells, pericytes, astrocytes and neurons (Fig. 2).

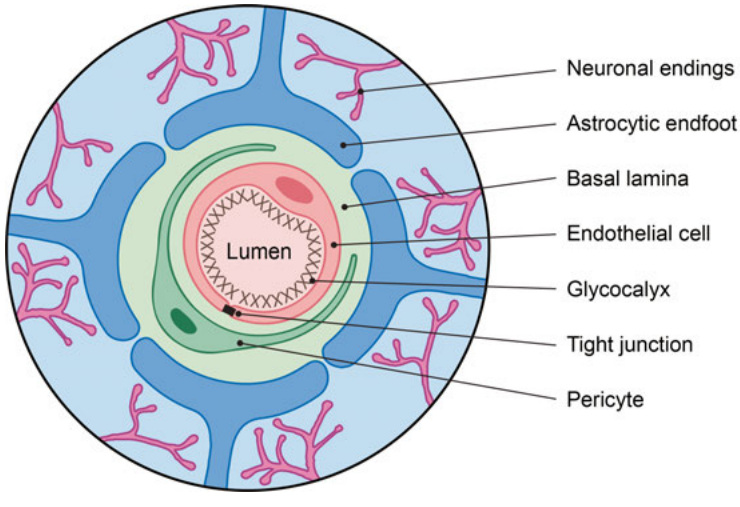

Figure 2. The neurovascular unit.

Brain endothelial cells are closely connected via tight junctions which contribute to the highly selective and semipermeable properties of the BBB[69]. The luminal side of the brain endothelial cells is coated with a negatively charged

sugar-protein mesh, called the glycocalyx, which helps lower cell permeability[70]. Pericytes play a crucial role in BBB development and maintenance as well as in transcytosis regulation[71,72]. Astrocytic endfeet surround brain vessels. They secrete factors that make up the basal lamina and influence permeability[70]. Astrocytes and neurons also interact together and with the brain endothelial cells to help regulate blood flow[73].

There are several pathways which molecules in the blood can follow to cross the BBB depending on the molecule's physical properties (Fig. 3)[64,66,67]. Small hydrophilic molecules can cross via paracellular diffusion through the tight junctions while small lipophilic molecules cross via transcellular diffusion. Positively charged large molecules (such as albumin or following engineered cationization) undergo adsorptive transcytosis[74]. Other large molecules, like insulin and transferrin (Tf), can cross the BBB via receptor-mediated transcytosis[64]. Many molecules cross with transport proteins. Some nutrients including glucose, amino acids, carbohydrates, hormones, fatty acids, and vitamins undergo carrier-mediated transport. Other small molecules can pass via active transporters which use adenosine triphosphate (ATP) as energy. Secondary active transporters, such as ATPases and cotransporters, maintain ion homeostasis in the brain. Primary active efflux transporters, such as the ATP-binding cassette transporters, transport molecules out of the endothelial cells and back into the blood. P-glycoprotein (also known as ABCB1) is an example of one such efflux transporter and plays a critical role in reducing the access of small hydrophobic drugs to the brain[75].

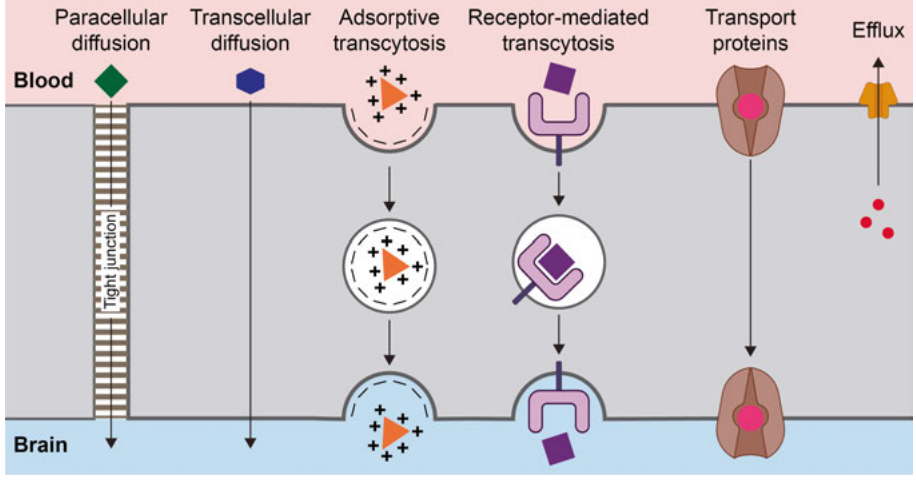

Figure 3. Transport routes across the BBB.

The molecular Trojan horse strategy

Since large biologics, including antibodies, do not passively cross the BBB efficiently, methods to increase their delivery into the brain have been a focus for the CNS drug development field. One popular approach is the "molecular Trojan horse" strategy wherein antibodies are engineered into bispecific antibodies with two targets: 1) the CNS target of interest and 2) a transport protein highly expressed on BBB endothelial cells[52,76]. In this way, antibodies can leverage the role of endogenous transporters or receptors undergoing receptor-mediated transcytosis to be carried across the BBB. This strategy has worked for shuttling large proteins into the brain with the TfR[64,77], CD98 heavy chain (a heavy chain of heterodimeric amino-acid transporters)[78–80], the insulin receptor[81–83], and the low-density lipoprotein receptor-related protein 1[84,85].

TfR and iron transport at the BBB

There are two homologues of TfR: TfR1 (also known as CD71) and TfR2. Together, they show ~45% identity in the amino acid sequences of the extracellular domains[86]. In humans, TfR1 is rather ubiquitously expressed and can be found on the surface of most cells. TfR2 is mainly present in tissues responsible for iron metabolism regulation, such as the liver and small intestine[86,87]. Tf has a higher affinity for TfR1 than TfR2[88,89]. Since TfR1 has a much higher expression level on brain endothelial cells than TfR2, TfR-mediated transcytosis research for therapeutic delivery to the brain has primarily concentrated on transport via TfR1. Therefore, this thesis will also focus on TfR1 and henceforth, TfR1 will be referred to as TfR.

TfR is a homodimer consisting of two 90 kDa subunits[90,91]. Each subunit contains a small intracellular domain, a transmembrane domain and an extracellular ectodomain. The ectodomain is further divided into three subdomains: the helical domain, the protease-like domain, and the apical domain (Fig. 4A). Aligning the amino acid sequences from the human, cynomolgus monkey, rat and mouse TfR ectodomains in UniProt (the Universal Protein Resource[92]) indicated that there is high homology between the two primate TfRs (91.1% identity) and the two rodent TfRs (91.4% identity) while primate and rodent TfRs only had ~73% shared identity. As animal models are frequently used in research, species specific differences in sequences can indicate how translatable a technique will be from bench to bedside[93].

A key function of brain endothelial TfR is to maintain iron homeostasis in both the brain parenchyma and brain endothelial cells. Iron is a critical molecule for living organisms because it plays a role in oxygen transport, enzyme reactions, redox reactions, cell division, the electron transport chain, and DNA synthesis[64]. TfR maintains homeostasis by transporting iron across the BBB into the brain or by loading iron into the endothelial cells, where it can be

stored for future. Two natural ligands of TfR which help with iron homeostasis are Tf and heavy-chain ferritin (H-Ft)[91,94].

The iron transport protein, Tf, is a 78 kDa monomeric glycoprotein arranged in two homologous lobes called the N- and C-lobes. Each lobe is composed of two subdomains (N_1, N_2, C_1, C_2) connected by a flexible hinge. Each lobe can bind a single iron atom with high affinity[95,96]. Tf has the capacity to carry two iron atoms and can thus exist in three forms: 1) apo-Tf when no iron is bound, 2) mono-ferric Tf when one iron atom is bound, and 3) di-ferric or holo-Tf, when both iron-binding sites are filled[91,95,97]. All three Tf states can bind to TfR with varying affinities in a pH-dependent manner. At physiological pH 7.4, holo-Tf binds to TfR stronger than mono-ferric Tf which binds stronger than apo-Tf. At endosomal pH 6.0, apo-Tf has the highest affinity to TfR with nearly irreversible binding[89,98]. Tf binds to the protease-like and helical domains of the ectodomain of a single TfR subunit[91,99]. Therefore, a functional dimeric TfR can bind to two Tf proteins and has the capacity to carry four iron atoms into a cell or across the BBB (Fig. 4B).

Holo-Tf binds to TfR on the luminal side of brain endothelial cells (Fig. 4C). This complex undergoes clathrin-mediated endocytosis and enters an early endosome. From there, TfR-mediated iron transport at the BBB can follow several pathways[64]. In one pathway, the early endosome containing the TfR/holo-Tf complex travels across the endothelial cells. The endosome docks on and fuses with the abluminal membrane and holo-Tf is released into the parenchyma. Intracellular tubules called sorting tubules have also been proposed to help regulate this pathway[100]. This transport pathway is currently the accepted mechanism of transcytosis for the molecular Trojan horse strategy[64]. The two other pathways that TfR can follow start with the early endosome progressing to a late endosome. As this occurs, the pH in the endosome continuously drops and iron bound to holo-Tf is released. The iron is transported into the cytoplasm where it can be used by the endothelial cell or stored for later[101]. The endosome with apo-Tf and TfR then follows one of two pathways: the recycling pathway or the degradation pathway. In the recycling pathway, apo-Tf and TfR are recycled back to the luminal membrane and apo-Tf is released into circulation[64,102]. In the degradation pathway, the endosome is further trafficked to the lysosome where TfR is degraded[100,102].

Ferritin is a large iron storage protein. The H-Ft in ferritin binds to TfR on the apical domain (Fig. 4D)[94]. It does not compete with binding of Tf, suggesting that these two proteins may co-regulate iron homeostasis. Upon binding to TfR, H-Ft is endocytosed. H-Ft is either transcytosed across the endothelial cells for iron delivery to the brain or trafficked to the lysosome where iron is released for cellular uptake[103]. Due to ferritin's large size and repetitive domains, it is thought that ferritin may bind two receptors at the same time, thus clustering receptors on the cell surface and likely inducing preferential trafficking to the lysosomes[104].

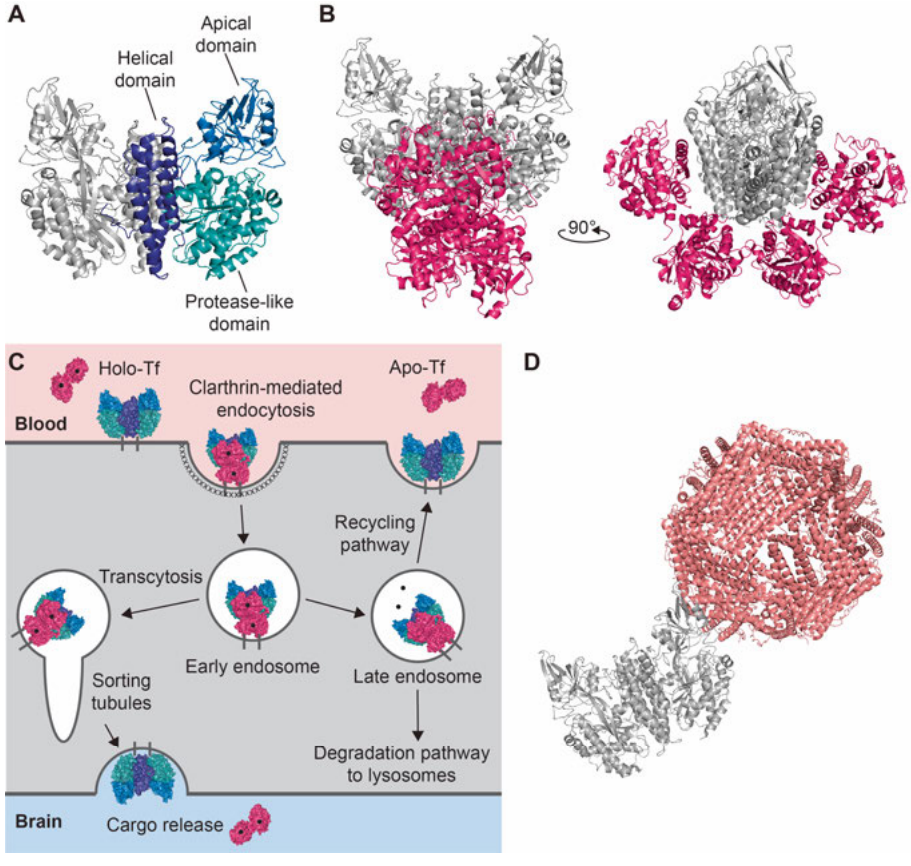

Figure 4. TfR and its endogenous ligands. (**A**) Ectodomain of the TfR homodimer (PDB: 1SUV) with one subunit in grey and the other coloured by domain[91]. (**B**) TfR can bind up to two Tf molecules (PDB: 1SUV). (**C**) The TfR/holo-Tf complex can follow alternative pathways after clathrin-mediated endocytosis. (**D**) TfR also binds to H-Ft (PDB: 6H5I)[94].

Applications of brain delivery with TfR binders

Although the exact transport mechanisms underlying the molecular Trojan horse strategy with TfR are uncertain, years of research in a range of species (mice[46,105–112], rats[113–116], non-human primates[117–119], and even some clinical trials[120–123]) indicate that targeting TfR can be an effective method for increasing brain delivery of therapeutic antibodies and peptides.

JCR Pharmaceuticals developed a recombinant iduronate-2-sufatase (IDS) enzyme replacement therapy for the lysosomal storage disorder, Hunter syndrome (or mucopolysaccharidosis II). Their drug, pabinafusp alfa (previously JF-141), is an IDS fused with an anti-human TfR antibody. It has produced positive results in phase I/II and II/III studies in Japan and a phase II study in

Brazil[120–122]. In March 2021, pabinafusp alfa was approved in Japan for treating Hunter syndrome[124] and is currently being tested in the global phase III STARLIGHT study (NCT04573023) in the USA, Brazil and Europe.

Denali Therapeutics has also developed an Fc (fragment crystallisable) domain with a binding region to human TfR[119,125]. They can use this specifically designed Fc domain to make transport vehicles for enzymes, antibodies, proteins or antisense oligonucleotides. They currently have three biotherapeutic drugs using this technology in clinical trials: DNL310, DNL593, DNL919. DNL310 is an enzyme transport vehicle with the IDS enzyme fused to the N-terminus of the engineered Fc domain for Hunter syndrome[125,126]. It is currently being tested in a phase I/II trial (NCT04251026) and the phase II/III COMPASS trial (NCT05371613). Interim data from the ongoing phase I/II study was presented at WORLDSymposium™ 2023. This data indicates that DNL310 is improving clinical symptoms in patients[127]. DNL593 is a protein transport vehicle where progranulin is fused to the TfR-binding Fc domain to treat frontotemporal dementia with *GRN* mutations[128,129]. There is an ongoing phase I/II trial (NCT05262023) testing the safety, tolerability, pharmacokinetics and pharmacodynamics of DNL593 in healthy participants and patients with frontotemporal dementia. Denali is also running a phase I trial (NCT05450549) in healthy participants to test the safety of DNL919. DNL919 is an antibody transport vehicle for treating AD. Here, the engineered Fc domain is fused to the $F(ab')_2$ of an anti-TREM2 antibody[130].

As mentioned previously, Roche has their own brain shuttle technology with a TfR-binding single chain Fab (fragment antigen binding). They have linked this Fab to the C-terminus of their anti-Aβ antibody to create trontinemab[46,47]. The first phase I trial (NCT04023994) with trontinemab in healthy participants finished in 2020. Although not published yet, Roche presented results at AD/PD2021 indicating that trontinemab is safe[131]. A phase I/II study (NCT04639050) with patients with mild to moderate AD began in 2021 and is still ongoing. Roche has also developed RG6035 or RO7121932, an anti-CD20 antibody with their brain shuttle technology for treating multiple sclerosis. The safety, tolerability, pharmacokinetics and pharmacodynamics of RG6035 is currently being tested in patients with multiple sclerosis in a phase I study (NCT05704361).

The TfR-mediated transcytosis strategy has also proven successful in the development of bispecific antibody-based radioligands for *in vivo* CNS PET and single-photon emission computed tomography (SPECT) imaging of intrabrain targets in AD mouse models and an alpha-synuclein deposition model for Parkinson's disease[61–63,132-143]. Bispecific antibody-based radioligands are more sensitive than the current small molecule tracers, such as [^{11}C]PiB, at detecting Aβ pathology. Compared to [^{11}C]PiB, immunoPET radioligands discriminate between AD and wild-type (WT) mice at an earlier disease state and detect reductions in Aβ levels in two mouse models more sensitively after an Aβ-reducing BACE-1 inhibition therapy[132,135,136,139]. Currently, the antibodies

used for immunoPET imaging in mice have slow pharmacokinetics thus requiring long-lived radionuclides, such as iodine-124 and zirconium-89. However, these are not suitable for clinical use. Recent research is therefore investigating how to improve the pharmacokinetics so immunoPET radioligands could be labelled with clinically relevant radionuclides such as fluorine-18[137]. Strategies have included protein engineering smaller molecules without an Fc[136,144], using clearing agents[141], and pretargeted imaging based on click chemistry[137,145]. Pretargeted imaging with click chemistry is a two-step strategy that takes advantage of the bioorthogonal, inverse electron demand Diels-Alder reaction. First, a trans-cyclooctene (TCO)-functionalized bispecific antibody would be injected into circulation. Once any unbound antibody has been eliminated from the body, an ^{18}F-labelled tetrazine with fast kinetics could be injected shortly before PET imaging.

Properties influencing TfR-mediated transcytosis

There are several criteria that should be considered when designing a TfR-binding, bispecific antibody. The construct must be stable and functional in a bispecific format in order to engage with the TfR, cross the BBB and still interact with the CNS target. Further, affinity to the CNS target needs to be stronger than the affinity to TfR to promote dissociation from TfR at the abluminal membrane and association with the CNS target[146,147]. Otherwise, the bispecific antibody risks staying bound to TfR and being ferried across the endothelial cells back to the blood[148]. The bispecific antibody should also not compete with endogenous TfR binders. This may help increase transcytosis of the bispecific antibody and will also decrease the chance of side effects by ensuring that the endogenous TfR ligands can still bind normally. For example, most anti-TfR antibodies studied bind the apical domain and therefore do not compete with Tf. In addition, the final purpose of the bispecific antibody should be kept in mind. For example, if it will be a PET radioligand to visualize Aβ aggregates or an anti-Aβ immunotherapy. A PET radioligand will be dosed lower than a therapeutic bispecific antibody. PET radioligands also require fast pharmacokinetics and would likely not benefit from Fc effector function. Conversely, therapeutic bispecific antibodies for AD commonly prefer slower pharmacokinetics and the method of action may require immune activation via Fc effector function once bound to Aβ aggregates.

Research into TfR-binding modules for BBB crossing has elucidated several properties that can influence transport efficiency.

Affinity is the strength of binding at a single site[149]. Thus, the affinity of a bivalent antibody is the strength of one arm binding to the antigen. Therapeutic bispecific antibodies display a bell-shaped relationship between affinity and brain delivery[106,107,115,117,150–153]. Antibodies with too high affinity are more

likely to follow the degradation pathway to the lysosomes in the brain endothelial cells. They can also lead to acute peripheral symptoms including first infusion reactions and reductions in reticulocyte count[150]. In contrast, antibodies with too low affinity bind insufficiently to TfR for transcytosis to occur and remain in the blood. However, this relationship may be related to **dose** such that at tracer doses, higher affinity results in higher brain uptake[106,151,154]. A **pH-dependent binding kinetic profile** with high affinity at physiological pH 7.4 and lower affinity at endosomal pH 6.0 could be beneficial for increasing transcytosis rates[155].

Evidence suggests that **valency**, or the number of times the construct binds to TfR, also plays a role. Monovalent TfR-binders shuttle cargo across the BBB more efficiently than bivalent binders and have reduced peripheral side effects[46,61,100,156,157]. Bivalent binders can cluster TfR on the surface of brain endothelial cells which drives endosomal trafficking towards lysosomal degradation and leads to decreased levels of TfR on endothelial cells even 48 h after injection[46,104,156]. Therefore, it is currently thought that the most efficient and safest binder for TfR-mediated transcytosis is a monovalent binder with medium-low affinity. However, bivalent anti-TfR antibodies can bind with both arms *in vivo* either to the same dimer or to two separate TfRs, giving them a stronger **apparent affinity (or avidity**) than the measured affinity for a single binding event. Monovalent binders generally have weaker apparent affinity to TfR than their bivalent parent antibodies[46,106]. It is currently unclear if the benefits of a monovalent binder are due to valency or the decreased apparent affinity or, as is more likely, a combination of both.

Size also impacts the pharmacokinetics such that smaller bispecific constructs are cleared from the blood and brain faster than larger variants[134,136,144,158]. This could be an optimal characteristic for immunoPET radioligands since the background signal from blood will be eliminated more quickly leading to improved contrast.

Methods

TfR-binding bispecific antibody production

Three anti-TfR antibodies were used throughout this thesis: 8D3, OX26, and 15G11. All of these antibodies bind to the TfR apical domain and have been shown to carry large molecules over the BBB in different species: 8D3 in mice, OX26 in rats and 15G11 in non-human primates and humans[114,159,160]. 8D3 and OX26 were first described as monoclonal antibodies for immunohistochemical staining of TfR in mice and rats respectively[161,162], while 15G11 was developed at Genentech (patent #US9708406)[160].

The anti-Aβ antibody, bapineuzumab (Bapi), binds with high affinity to the first 5 amino acids on the N-terminus of Aβ and does not discriminate between Aβ aggregate species[163]. Bapi was the first passive immunotherapy targeting Aβ to reach phase III clinical trials. The phase III trials were terminated in part due to adverse effects such as amyloid-related imaging abnormalities[164,165]. Bapi was used throughout the thesis as the standard Aβ binder since it binds all Aβ species monovalently.

Different methods were used throughout the thesis for producing antibodies, Fab fragments, and bispecific antibodies. Recombinant antibodies were produced using the Expi293 Expression System in **Papers I** and **II** and the ExpiCHO Expression System in **Papers III** and **IV**.

In **Paper II**, 8D3 and 15G11 Fab fragments were produced recombinantly while OX26 Fab fragments were generated with the protease, papain. In a high cysteine concentration buffer, papain digests the Fc domain of an IgG leaving two Fab fragments (Fig. 5A).

In **Paper I**, bispecific fusion proteins were produced by chemically conjugating the OX26 antibody to Bapi $F(ab')_2$ fragments. First, Bapi was cleaved into a $F(ab')_2$ fragment with the cysteine protease, IdeS (Genovis AB). IdeS produces a homogenous preparation of $F(ab')_2$ fragments by cleaving a human IgG at a specific site below the hinge region (Fig. 5A). Then, the TCO-modified OX26 antibody was chemically conjugated to the tetrazine-modified Bapi-$F(ab')_2$ via an inverse electron demand Diels-Alder reaction. (Fig. 5B).

Affinity variants in **Papers I**, **III**, and **IV** were produced by introducing single alanine point mutations in the complementarity determining regions of the anti-TfR antibodies. Alanine point mutations are beneficial for altering affinity because these mutations remove any side chains past the β carbon without affecting the main peptide chain conformation[166].

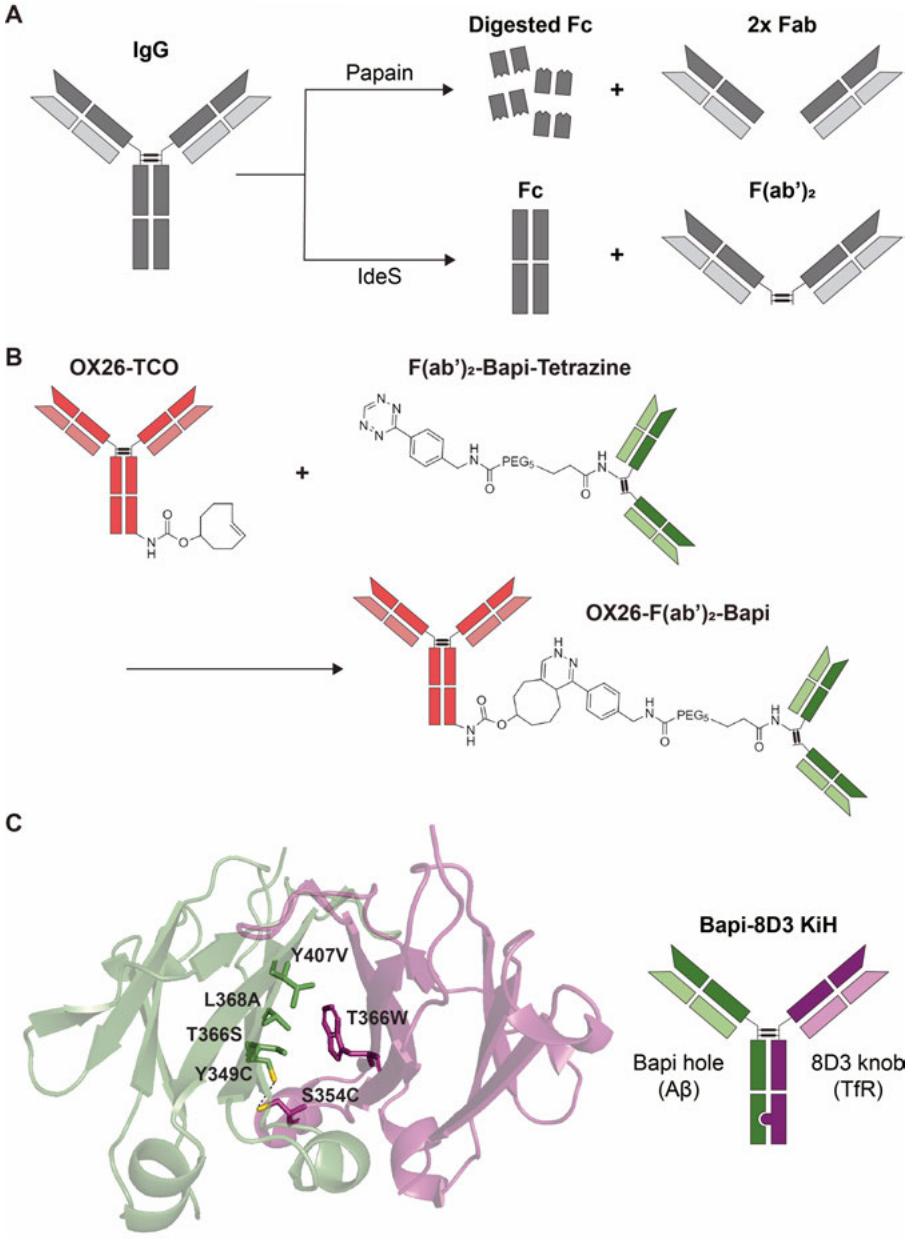

Figure 5. Methods to generate bispecific antibodies. (**A**) Full-length IgG antibodies were enzymatically cleaved with papain or Ides to produce 2 Fab fragments or a F(ab')$_2$ fragment, respectively. (**B**) The bispecific fusion protein, OX26-F(ab')$_2$-Bapi, was produced with chemical conjugation. (Adapted from Bonvicini and colleagues[167].) (**C**) KiH heterodimerization mutations to generate monovalent, bispecific antibodies (PDB:4NQS)[168].

A knob-into-hole (KiH) design was used to generate full-length, monovalent, bispecific antibodies in **Papers III** and **IV** (Fig. 5C). KiH heterodimerization

technology involves replacing a small amino acid in one C_H3 domain with a larger one to form a "knob" (T366W) and replacing large amino acids in the other C_H3 domain with smaller ones to form a "hole" (T366S/L368A/Y407V)[169]. The smaller amino acids in the hole C_H3 domain form a hydrophobic pocket that thermodynamically favours heterodimer formation with the knob C_H3 domain. Here, a disulphide bond was also introduced (S354C on the knob C_H3 domain, Y349C on the hole C_H3 domain) to improve heterodimer yields by enhancing stability[170]. To prevent mispairing of the different light chains, the knob and hole half-antibodies were produced separately and assembled into bispecific antibodies following purification from the cell supernatant[171]. This design ensured that the antibodies could differ in valency to TfR while keeping the size and Fc region constant.

The Fc region on IgG antibodies can activate the immune system via effector functions. Fc binding to Fc-gamma receptors (FcγR) on effector cells activates antibody-dependent cellular cytotoxicity (ADCC) or antibody-dependent cellular phagocytosis (ADCP) while Fc binding to complement protein 1q (C1q) activates complement-dependent cytotoxicity (CDC)[172]. Fc effector function can lead to unwanted side effects such as first infusion reactions and reduction in reticulocytes[47,150]. Immune activation is not required nor desired for immunoPET radioligands. Therefore, effector function was silenced in antibodies in **Papers III** and **IV** by introducing the L234A/L235A/P329G (LALA-PG) mutations in the C_H2 domain[173]. L234 and L235 are part of the FcγR binding site and P329 is part of the C1q binding site[174]. The LALA-PG mutations thus effectively reduce ADCC and CDC while maintaining antibody stability[173,175].

Affinity determination

Different techniques can measure affinity or apparent affinity depending on the assay.

Biacore surface plasmon resonance (SPR)

Developed nearly 30 years ago, SPR is a highly sensitive and accurate method for measuring affinity (K_D) and kinetic rate constants (k_a and k_d)[176]. Generally, it involves one protein, the ligand, being immobilized to a dextran matrix on a gold-coated sensor chip and the analyte being flown over in solution. A light is shone through a prism on the opposite side of the chip surface and is reflected off the chip. Photons from the light interact with electrons in the gold which gives rise to an evanescent wave of surface plasmons. As analyte binds to the ligand, the refractive index of the sensor surface changes and, in turn, the angle of reflected light shifts. The ever-shifting reflection angle is detected and displayed as response units in Biacore SPR.

The classic set up when measuring the affinity of an antibody to its antigen is to have the antibody as the ligand and the antigen as the analyte and to fit the data with a 1:1 binding model (Fig. 6A). This works if the antigen is a monomer with only a single epitope and thus, can only bind to the antibody once. However, if the antigen forms multimers or has multiple epitopes, the binding stoichiometry can increase which results in avidity. To counter this, the antigen can be the ligand and a Fab or antibody can be the analyte (Fig. 6B). Analysis of binding with the antibody as the analyte and a 1:1 binding model yields the apparent affinity.

In **Paper II**, we thoroughly explored and compared different Biacore assays with the antibody as either the ligand or the analyte. Biacore was also used in **Paper I** as a quality control of our OX26 affinity variants and in **Paper IV** for the initial screen of our monovalent and bivalent affinity variants.

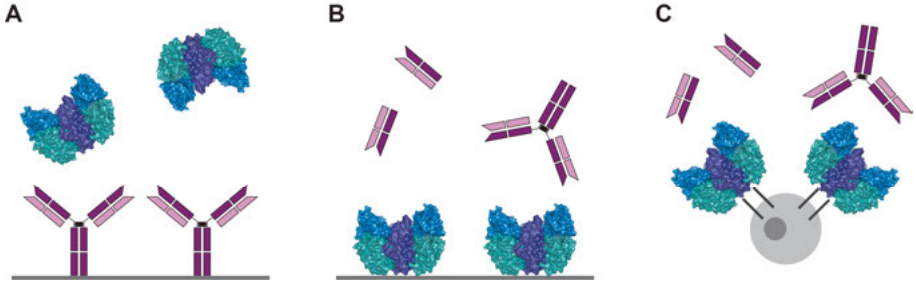

Figure 6. Assays for measuring antibody affinity to TfR. (**A**) Biacore setup with the anti-TfR antibody as the ligand and TfR as the analyte. (**B**) Alternative Biacore setup with TfR as the ligand and the Fab or antibody as the analyte. (**C**) An on-cell affinity determination assay.

On-cell affinity determination assay

An apparent affinity can also be determined by assessing binding to cells presenting the antigen of interest (Fig. 6C)[177]. Binding of antibody at various concentrations to the cell surface is detected with flow cytometry which yields an EC50 value. The EC50 value can be an estimate for apparent affinity since binding site saturation is the maximum response measured in the assay. Although on-cell assays are not able to determine the kinetic parameters of an interaction, they provide unique *in vitro* conditions that mimic the *in vivo* receptor density, conformation and orientation[177]. In **Paper II**, we compared an on-cell assay for measuring apparent affinity of anti-TfR antibodies to the various Biacore assays. The on-cell assay was also used in **Papers III** and **IV**.

Enzyme-linked immunosorbent assay (ELISA)

ELISA is a common, sensitive biochemical method based on interactions between antibodies and antigens. In an indirect ELISA, the antigen is coated on

the plate surface and binding strength of an antibody is assessed. Affinity to Aβ was measured in **Paper III** with an indirect ELISA. Indirect ELISAs were also used in **Papers I**, **III** and **IV** as quality control to assess possible impacts of the radiolabelling reaction on binding to TfR or Aβ.

Sandwich ELISAs can be used to determine the concentration of an antigen. The concentration of various Aβ species in rat brain homogenates were measured in **Paper I** with sandwich ELISAs.

Animal models

Animal models are commonly used in biomedical research.

Experiments in **Paper I** were performed on WT Fischer 344 and TgF344-AD rats with abundant Aβ pathology. TgF344-AD rats express human *APP* with the Swedish mutation (*KM670/671NL*) and human *PSEN1* with exon 9 deletion and are maintained on a Fischer 344 background. This transgenic rat model displays an onset of age-dependent Aβ plaque pathology at 6 months and a significantly higher [^{18}F]Florbetaben-positive plaque load than WT rats at 18 months[178,179].

In **Papers III** and **IV**, WT C57BL/6 mice were used for the pharmacokinetic experiments. Aged $App^{NL\text{-}G\text{-}F}$ mice were also included in the pharmacokinetic experiments in **Paper III**. In the $App^{NL\text{-}G\text{-}F}$ model, the mouse *APP* gene has been genetically altered to include the human Aβ amino acid sequence with the Swedish (*KM670/671NL*), Arctic (*E693G*), and Iberian (*I716F*) mutations. In contrast to transgenic models where the human gene is inserted randomly into the genome, knock-in models, such as the $App^{NL\text{-}G\text{-}F}$ model, express the gene at the natural site in the genome. $App^{NL\text{-}G\text{-}F}$ mice are characterized by rapid accumulation of Aβ pathology that consists mainly of $Aβ_{1\text{-}42}$ and can be visualized with immunohistochemistry already at 2-3 months of age[180,181].

Capillary depletion

Pharmacokinetic studies were performed in **Papers I**, **III**, and **IV** to evaluate the biodistribution of the injected antibodies. Part of this analysis included capillary depletion. Capillary depletion was first published in 1990 and has become a common technique when studying transport of bispecific proteins across the BBB[46,107,113,144,154,182,183]. It enables separation of total brain signal into the portion that has truly crossed into the parenchyma and the portion that is still in the endothelial cells. Density gradient centrifugation of a brain homogenate in a polysaccharide solution was employed to separate the brain capillaries and parenchyma. After centrifugation, there were three fractions:

1) a fatty layer containing myelin, 2) a supernatant fraction containing parenchymal cells, and 3) a microvasculature-enriched pellet. The first two fractions were combined to form the parenchymal supernatant analysed in this thesis.

Radiochemistry

In **Papers I**, **III**, and **IV**, antibodies were radioiodinated by the direct iodination Chloramine-T method. This labelling is based on the electrophilic attack of oxidized iodine to the phenolic rings of the tyrosine residues[184]. The reaction was quenched with the addition of the reducing agent, sodium metabisulphite.

In **Paper I**, bispecific fusion proteins were radiolabelled with iodine-124 (^{124}I) or iodine-125 (^{125}I). Antibodies in **Papers III** and **IV** were labelled with iodine-125.

Iodine-124 has a half-life of 4.2 days and undergoes beta decay: 74.1% as electron capture and 22.4% as positron emission[185]. The data correction abilities of modern PET scanners make iodine-124 a suitable isotope for preclinical PET experiments. However, it is not optimal for clinical use due to its relatively long half-life, low fraction of positron emission, and likelihood to accumulate in the thyroid.

Iodine-125 has a much longer half-life at 59.5 days. It decays only by electron capture to an excited state of tellurium-125 which then further decays into the ground state of tellurium-125 via gamma emission[186]. Iodine-125 is not suitable for PET since it does not undergo beta decay. However, its long half-life and detectability in gamma counters make it a good isotope choice for biodistribution studies.

PET

PET imaging was performed on rats in **Paper I** to assess if antibody-based Aβ PET could be translated from mice, a species that had been studied extensively.

In PET imaging, a radioligand is injected which has two key characteristics: it binds to a biological target and it has a radionuclide that undergoes positron decay[186]. The radionuclide allows for the detection of the radioligand's distribution in the body. As it decays, the radionuclide releases a positron that annihilates with an electron (Fig. 7). The annihilation produces two high-energy gamma photons (511 keV each) which are emitted at 180° from each other. These photons are then detected on opposing detectors, creating a coincidence event. The PET scanner has a ring of detectors and uses multiple coincidence events to calculate the location and amount of radioactive decay is emitted

from the radioligand. Thus, PET is quantitative as the amount of radioactivity measured correlates with the amount of biological target of interest.

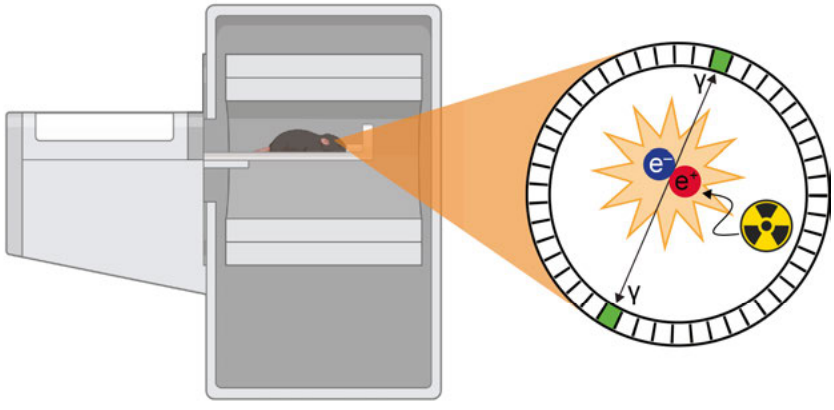

Figure 7. The basic principle of PET imaging. The radionuclide emits a positron (e^+) which annihilates with an electron (e^-) to produce two gamma photons (γ). These photons are detected by the PET detector ring as a coincidence event.

The spatial resolution of a PET scan is determined to a certain extent by the radionuclide used. Different PET radionuclides emit positrons at different energies and this energy determines the distance a positron will travel before it annihilates with an electron. The further a positron travels, the more difficult it is for the PET scanner to back calculate the location of decay, thus reducing the spatial resolution. For example, carbon-11, fluorine-18, copper-64, and zirconium-89 are considered short-range positron emitters with a mean range of 0.6-1.3 mm while nitrogen-13, oxygen-15, gallium-68, and iodine-124 are considered long-range positron emitters with a mean range >1.5 mm[185].

Ex vivo autoradiography

Ex vivo autoradiography is a technique that allows visualization of previously injected radioactive ligands in tissue sections[187]. Throughout this thesis, *ex vivo* autoradiography was performed on perfused animals. The perfusion step removes any background signal originating from the blood so only the remaining radioactive signal bound in the brain is imaged.

In **Papers I** and **III**, *ex vivo* autoradiography was compared with immunohistochemical stainings of Aβ pathology to visualize the spatial distribution of injected antibody in the brain relative to Aβ pathology. *Ex vivo* autoradiography and Aβ immunohistochemistry were also used in **Paper I** to confirm the origin of the signal observed in the *in vivo* PET scans.

Aims

The overall aim of this thesis was to evaluate binding properties to TfR for optimized brain delivery of preclinical Aβ immunoPET radioligands.

Specific aims

I. To determine if Aβ pathology in an AD rat model can be visualized with immunoPET and to evaluate the effect of TfR affinity on brain uptake at a tracer dose.

II. To compare several Biacore assays and an on-cell assay for measuring antibody affinity to TfR.

III. To investigate how TfR affinity affects brain uptake of bispecific antibodies at a tracer dose in both WT and $App^{NL\text{-}G\text{-}F}$ mice.

IV. To evaluate the effect of valency on TfR-mediated transcytosis of antibodies across the BBB when apparent affinity is controlled.

Results and discussion

CNS immunoPET with TfR delivery is translatable

Brain delivery of therapeutic biologics via the TfR is well established to translate across species from mouse to rats to non-human primates to humans[107,111,115–117,119,123]. Conversely, PET of a CNS target using trace amounts of radiolabelled TfR-binding antibodies has only been attempted in mice[61-63,132-143]. Furthermore, the necessary pharmacokinetic properties are different for a therapeutic antibody and an immunoPET radioligand. Thus, the first aim of this thesis was to investigate if PET imaging of Aβ with an antibody-based radioligand could be translated to another species besides mice. In **Paper I**, we attempted to image Aβ pathology in rats with our bispecific fusion protein, [^{124}I]I-OX26$_5$-F(ab')$_2$-Bapi.

Three days post-injection of [^{124}I]I-OX26$_5$-F(ab')$_2$-Bapi, there was a significantly higher PET signal in all brain regions measured in TgF344-AD rats compared with WT littermates. This was supported by the *ex vivo* autoradiography which showed substantially higher radioactive signal in the transgenic animal brains compared to the near background signals in WT animals. Furthermore, the regions with high radioactivity, specifically the cortex and cerebellum, localized very well with Aβ_{1-42} pathology in immunohistochemical stainings. The PET signal also correlated with Aβ_{1-40} and Aβ_{1-42} measured with a biochemical ELISA assay.

Taken together, these findings show that bispecific antibody-based PET imaging of brain Aβ pathology using TfR-mediated transport was successful at differentiating between transgenic AD model rats and WT rats. [^{124}I]I-OX26$_5$-F(ab')$_2$-Bapi is a promising candidate for Aβ PET in rats which creates opportunities to pursue antibody-based PET in AD rat models. Furthermore, not only was immunoPET imaging of Aβ successful in rats but it reflected the previous findings in mice that immunoPET imaging is more sensitive than small molecule tracers at detecting Aβ pathology[132,135,136,139]. Therefore, this PET imaging strategy was translatable from mice to rats and could likely be translated from bench to bedside with the correct human TfR-binder.

Measuring affinity to TfR

Despite the field's agreement that affinity influences transcytosis efficiency at therapeutic doses and the years of research focusing on TfR-mediated brain delivery, there is no accepted method for how to best measure TfR affinity. Affinities presented in literature have been determined with a range of methods including Biacore, Octet, inhibition ELISA, and radio-receptor assays on cells[61,105,107,115,130,160,183,188,189]. Thus in **Paper II**, we assessed the affinity of three antibodies in four different Biacore setups: antibody capture (Fig. 8A), TfR immobilization (Fig. 8B), TfR capture via a FLAG-tag (Fig. 8C), and TfR capture via immobilized holo-Tf (Fig. 8D). The results from the Biacore setups were compared to the apparent affinities measured in an on-cell affinity assay as cell assays tend to mimic *in vivo* parameters (Fig. 8E)[177].

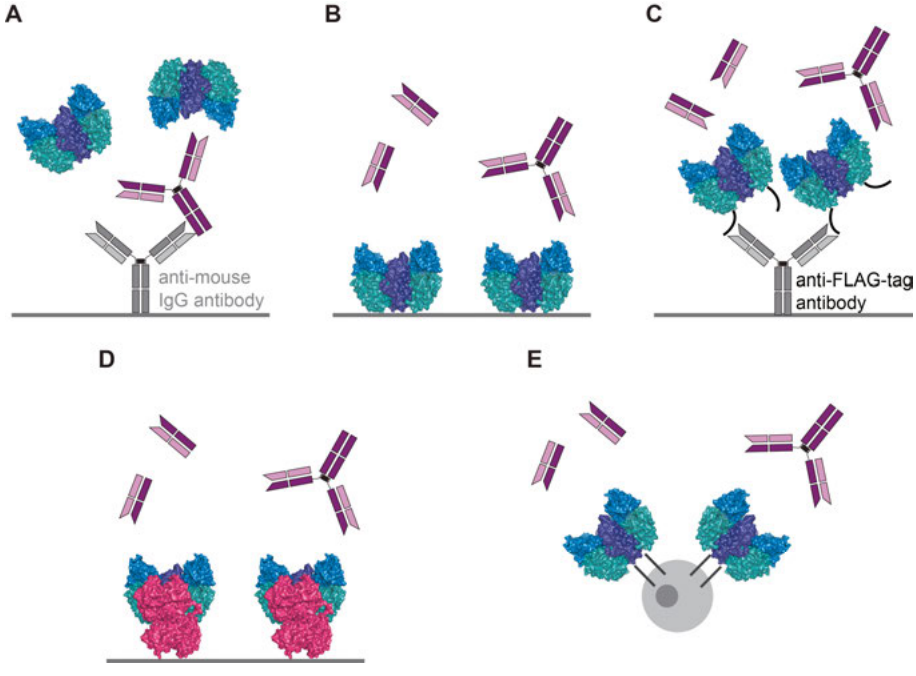

Figure 8. Biacore and on-cell assays assessed in **Paper II**. Biacore assays where (**A**) the anti-TfR antibody is captured, (**B**) TfR is immobilized and either the Fab or antibody is the analyte, (**C**) TfR with an N-terminal FLAG-tag is captured via an anti-FLAG-tag antibody and (**D**) TfR is captured via immobilized holo-Tf. (**E**) An assay performed on cells determines the apparent affinity to TfR.

In the antibody capture setup, the apparent affinity of rat TfR to OX26 was similar to the affinities presented in literature[115,189]. The apparent affinity of human TfR binding to 15G11 was slightly stronger than the previously reported affinity and the apparent affinity measured in the on-cell assay[160]. Mouse TfR binding to 8D3 however, had a substantially higher affinity than

previously reported values and the on-cell apparent affinity. This discrepancy was primarily driven by a slower dissociation rate constant[107]. Thus, we hypothesize that the difference in the measured and previously reported affinities may be due to TfR forming dimers during the experiment leading to an avidity effect.

Therefore, we tested if having TfR as the ligand would circumvent this avidity effect. This switch in setup resulted in substantially lower apparent affinity for 8D3 confirming that it did help. The 8D3 and 15G11 Fab affinities measured in the immobilized TfR setup matched the apparent affinities from the on-cell assay while the antibodies had slightly stronger affinities in Biacore. This suggests that this Biacore setup is better suited for measuring the affinity to TfR of monovalent but not bivalent binders.

We then wanted to assess whether a more uniform surface would further improve the relatability of the Biacore measurements to the on-cell values. In the TfR immobilization setup, TfR was immobilized via NHS-coupling which creates a heterogenous surface. To obtain a directed capture of TfR, we tried two approaches: the FLAG-tag capture of TfR and the capture of TfR with its endogenous ligand, holo-Tf. The FLAG-tag capture setup was the only setup to yield apparent affinities similar to the on-cell apparent affinities for both the antibody and the Fab fragment. This indicated that it may yield apparent affinities that could translate *in vivo* with the added benefit of measuring the kinetic rate parameters as well. The setup with the holo-Tf capture of TfR did not yield as similar apparent affinities to the on-cell results. However, this setup may still be useful for assessing competition between the antibody and Tf when binding to TfR.

Although the FLAG-tag capture setup was determined to be the preferred setup for measuring affinity in Biacore, it was not possible to get a functional surface with the FLAG-tag mouse TfR. The capture levels were too low and a preliminary analysis of bivalent 8D3 yielded very noisy sensorgrams and high variation in affinity. Therefore, we continued with the on-cell assay in **Paper III** since we hypothesize that this assay also mimics *in vivo* conditions. One limitation of the on-cell assay is that it is not high-throughput. This did not pose an issue for **Paper III** since we had a limited number of antibodies to evaluate. It was however an issue for **Paper IV** as we initially had 12 monovalent variants and 29 bivalent variants. Therefore, we started the *in vitro* scan with the immobilized TfR setup in Biacore. However, we ran into unexpected technical complications. Immobilized mouse TfR seemed to be unstable and sensitive to repetitive regeneration. This method likely requires further optimization to be a high-throughput assay as Biacore is intended to be. Despite the challenges, we were able to narrow down the possible variants to an acceptable number for on-cell affinity determination. In the on-cell assay, we identified two pairs of monovalent and bivalent antibodies with similar apparent affinity: 1) Bapi-8D3$_{WT}$ and 8D3$_{D54A/Y92A}$ with an affinity around 10 nM

and 2) Bapi-8D3$_{Y52A/Y92A}$ or Bapi-8D3$_{Y52A}$ and 8D3$_{D54A/Q90A}$ with an affinity around 250 nM.

Affinity effects on TfR-mediated brain delivery are dose-dependent

Affinity to TfR affects the efficiency of brain delivery for therapeutic biologics. However, therapeutics are typically dosed at 1-50 mg/kg while tracer doses for antibody-based radioligands are less than 1 mg/kg. Some reports have indicated that the effects of affinity shift at tracer doses so that higher brain concentrations are obtained with higher affinity binders[106,151,154]. We investigated the influence dose has on affinity effects in **Papers I** and **III**.

In both papers, we found that the higher affinity binder had higher brain uptake 4 h post-injection. In **Paper I**, we had two affinity variants of the anti-rat TfR antibody, OX26: OX26$_5$ which had a 5 nM affinity for rat TfR and OX26$_{76}$ which had a 76 nM affinity for rat TfR. After the chemical conjugation to produce our two bispecific fusion proteins, the affinity measured *in vitro* to Aβ protofibrils was unaffected. The affinity for rat TfR was also unaffected for OX26$_5$-F(ab')$_2$-Bapi but was substantially lower for OX26$_{76}$-F(ab')$_2$-Bapi. OX26$_5$-F(ab')$_2$-Bapi was taken up into the brain at a much higher extent than OX26$_{76}$-F(ab')$_2$-Bapi 4 h post-injection of a 0.04 mg/kg dose in WT rats. However, it was unclear if the lower uptake of the lower affinity variant was because of the lower dose or because the affinity of OX26$_{76}$ was reduced to such an extent after chemical conjugation that it bound to TfR insufficiently *in vivo* for transcytosis.

These results prompted a thorough investigation in **Paper III** with three affinity variants of 8D3 in a bispecific format (Bapi-8D3$_{WT}$: 10.0 nM, Bapi-8D3$_{Y32A}$: 19.6 nM, Bapi-8D3$_{Y52A}$: 241 nM) and the non-TfR-binding Bapi at a tracer dose of 0.2 mg/kg in both WT and *App*$^{NL-G-F}$ mice. Throughout **Paper III**, the two stronger TfR-binders, Bapi-8D3$_{WT}$ and Bapi-8D3$_{Y32A}$, had similar pharmacokinetics independent of genotype. Blood pharmacokinetic profiles were similar between antibodies but there was a trend of faster blood elimination with increased TfR affinity. Brain uptake at 4 h post-injection was dependent on affinity, but not genotype: both Bapi-8D3$_{WT}$ and Bapi-8D3$_{Y32A}$ had higher brain uptake than Bapi-8D3$_{Y52A}$, which, in turn, had higher uptake than Bapi. Brain exposure profiles overtime were dependent on genotype such that brain concentrations decreased in WT animals and initially increased and plateaued in *App*$^{NL-G-F}$ mice. The *ex vivo* autoradiography reflected the brain pharmacokinetic data. The autoradiography and immunohistochemistry in adjacent sections from *App*$^{NL-G-F}$ mice also provided information on the spatial distribution of the antibodies relative to the Aβ pathology in the brain. The two

stronger TfR binders were evenly distributed throughout the brain and co-localized well with Aβ pathology. Bapi localized in hotspots near the ventricles in the autoradiography which did not reflect the spread of the pathology well and was characteristic of non-TfR binding antibodies[62,63,138,190]. The weakest TfR binder, Bapi-8D3$_{Y52A}$, had a blend of both distribution patterns: it had an even, albeit low, distribution with hotspots.

Overall, these results corroborate the current hypothesis that the effect of affinity on TfR-mediated transcytosis is dose-dependent[106,151,154]. At therapeutic doses, there is an optimal affinity range where higher and lower affinities do not cross the BBB well (Fig. 9). However, the similar pharmacokinetics seen here with the two high affinity antibodies is also in line with the literature[106]. Taking the results presented here and from literature, it may be that at tracer doses, higher affinity leads to higher brain uptake but that there is a range of affinities where the affinity effect plateaus (Fig. 9).

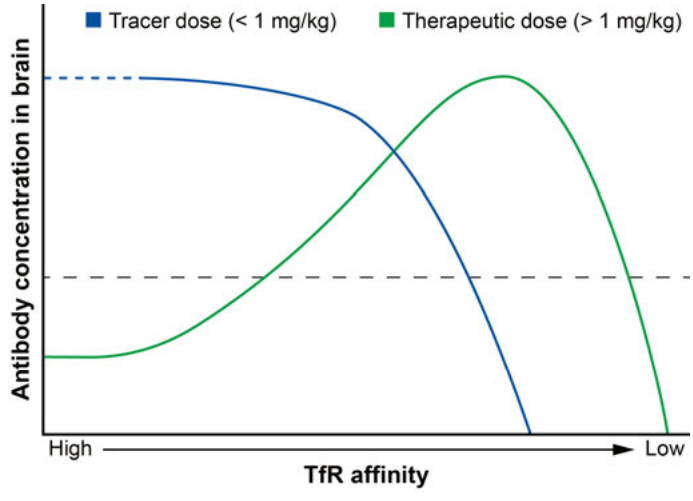

Figure 9. Proposed relationship between TfR affinity and antibody concentration in brain tissue at a tracer dose (blue line) and a therapeutic dose (green line). The black dashed line represents the brain concentration threshold required for adequate imaging or therapeutic effect. (Adapted from Yu and colleagues[117].)

Many of the previous, successful immunoPET radioligands studied have retained the Fc effector function, including [^{124}I]I-OX26$_5$-F(ab')$_2$-Bapi from **Paper I**[61,106,132,138]. Although they could differentiate between animals with and without pathology in PET scans, the concentrations of these bispecific antibodies in the brain declined overtime. We hypothesize that the continued maximal retention of antibody concentrations in the brain in *App*$^{NL-G-F}$ mice over one week post-injection was due to the loss of effector function. Further sup-

porting this hypothesis, other antibody-based radioligands with reduced effector function or no Fc have shown similar pharmacokinetic profiles as the antibodies in **Paper III**[63,136,142].

Valency effects on brain delivery are independent of apparent affinity

Monovalent binding to TfR is also well-accepted to be critical for efficient brain delivery of biologics via the TfR since bivalent binders tend to be sorted for lysosomal degradation[46,61,100,156,157]. The evidence for this claim is mostly based on studies comparing monovalent and bivalent forms of the same antibody but antibodies typically have a stronger apparent affinity in the bivalent form than the monovalent form[46,106]. Since affinity affects the extent of brain delivery, it is unclear if the valency effects reported are actually due to valency and not simply apparent affinity.

In **Paper IV**, we aimed to investigate this question by pairing monovalent and bivalent variants of 8D3 with the same apparent affinity. We identified two apparent affinity pairs and tested the pair with the stronger apparent affinity, Bapi-8D3$_{WT}$ and 8D3$_{D54A/Y92A}$, in WT mice at a tracer dose of 0.2 mg/kg. Both antibodies had similar blood pharmacokinetic profiles during the 4 h post-injection. Significantly more monovalent antibody was retained in the brain 4 h post-injection than the bivalent antibody. Unexpectedly though, the low brain uptake of the bivalent antibody was not supported by an increased retention of bivalent antibody in the capillary fraction. In fact, when normalized to the total signal of both capillary depletion fractions, both antibodies had the same distribution between the fractions with ~20% in the capillaries and ~80% in the parenchyma. One possible explanation is that at the tracer dose, the lysosomal degradation pathway was not saturated. Thus, the rate of bivalent antibody degradation was such that the antibody did not have the chance to accumulate in the capillaries. Since the antibodies were labelled with a non-residualizing radionuclide (i.e. iodine-125), degraded antibody would not be detectable[191].

Conclusions and future perspectives

In conclusion, antibodies are beneficial PET radioligands since they can have high specificity and selectivity to targets, such as a specific aggregated protein. A current challenge for applying them for CNS PET is that they do not passively cross the BBB well but this can be ameliorated by binding to the TfR. Properties affecting brain delivery via the TfR have been evaluated at therapeutic doses but radioligands are dosed substantially lower. The work presented in this thesis evaluated the effects of affinity, valency, and dose on the delivery of preclinical Aβ antibody-based PET radioligands to the CNS via the TfR.

In **Paper I**, we showed that an immunoPET radioligand using TfR-mediated brain delivery could sensitively differentiate between rats with and without Aβ pathology. This was the first time to our knowledge that hijacking of TfR was used in another species besides mice to deliver an immunoPET radioligand to image a target in the CNS. This suggests that the Trojan horse strategy for ferrying antibody-based radioligands to the CNS could eventually be applied for clinical use. However, this will require the development of a radioligand with a suitable human TfR antibody.

Affinity to TfR is one property that heavily influences delivery of biologics to the CNS. In **Paper II**, we described four Biacore setups and one on-cell assay for determining apparent affinities to TfR. Absolute affinity determination was challenging since assay orientation, surface capture methods, and antibody format can all impact the kinetic parameters measured in Biacore. All three setups described with TfR as a ligand seem to yield reliable relative affinities for antibodies and the specific question will likely determine which method is best. The setup with FLAG-tag captured TfR yielded the most similar apparent affinities to the on-cell assay. Therefore, a directional, uniform capture of TfR in Biacore may be optimal since it determines the kinetic parameters and mimics *in vivo* receptor conditions. Further optimization of the antibody capture and immobilized TfR setups could be performed. For the antibody capture setup, reducing the avidity measured for mouse TfR could be assessed by titrating down the levels of 8D3 captured or by having a different version of TfR, for example the isolated apical domain[130,192,193]. Optimization for the immobilized TfR setup could also include titrating down the levels of TfR immobilized on the surface to improve the apparent affinities

for bivalent antibodies. One could also investigate different regeneration solutions to assess improving surface stability overtime.

In **Papers I** and **III**, we concluded that stronger affinity to TfR yields higher brain delivery when the antibodies are administered at a tracer dose. The antibodies in **Paper III** were also lacking effector function. The resulting pharmacokinetic profiles in the $App^{NL\text{-}G\text{-}F}$ mice versus in the WT mice indicated that loss of effector function may be beneficial for target accumulation of an antibody-based radioligand. Future studies could further evaluate the effects of effector function on brain elimination when there is an intrabrain target present. This could be done by investigating the extent of microglial activation after injection of antibodies with or without ablated effector function.

Finally, in **Paper IV**, we produced and screened a novel library of 8D3 affinity variants in monovalent and bivalent formats. We identified two pairs of monovalent and bivalent antibodies that have similar apparent affinities. Administration of the stronger affinity pair to WT mice provided supportive evidence that monovalent binding yields higher brain uptake at a tracer dose. However, it was unclear from the capillary depletion if this was due to the bivalent antibody being trafficked to the lysosome for degradation. One could investigate the fate of the antibodies more extensively with several different techniques including: dual labelling with a residualizing (e.g. zirconium-89 or indium-11) and a non-residualizing (e,g. iodine-125) radionuclide, *in vivo* two-photon imaging of pHrodo-conjugated antibodies, *ex vivo* super resolution microscopy techniques, or *in vitro* live-cell imaging. One could also use western blot to determine the extent of TfR down-regulation in the capillary fraction. Other future studies could investigate the extent to which avidity affects bivalent binders by including the bivalent $8D3_{WT}$. Evaluation at therapeutic dosing could also be interesting to see if the valency effect on TfR-mediated transcytosis is exacerbated with increasing dose.

The conclusions of this thesis emphasize that the purpose of a bispecific antibody should be kept in mind during the design phase. An immunoPET radioligand which will be administered at a low, tracer dose will likely benefit from a monovalent design, with high affinity to TfR and ablated effector function. Hopefully, the work presented here will provide valuable insight for the development of an Aβ immunoPET radioligand for clinical use.

Popular science summary

Alzheimer's disease is the most common form of dementia. It is a neurodegenerative disease characterized by loss of memory and declining cognitive function. The underlying cause of Alzheimer's disease is thought to be proteins that unnaturally clump together to form aggregates: amyloid-β aggregates outside cells (called plaques) and tau aggregates inside cells (called tangles). These aggregates build up in the brain well before the typical clinical symptoms appear in patients. Amyloid-β first clumps into small aggregates and continues into larger and larger aggregates, eventually forming plaques. The smaller aggregates are considered to be more toxic than the plaques as they cause neuronal cell death. The more small aggregates there are in the brain, the worse a patient's memory loss usually is. Being able to detect these proteins before symptoms appear is critical for improving the chances of success of the therapies presently available to patients.

A current diagnostic method for Alzheimer's disease is positron emission tomography (PET) imaging. In PET imaging, a radioactive molecule (or radioligand) is injected into the patient at a very low dose. The radioligand will bind to the target of interest in the patient. The distribution of the radioligand is detectable by the PET scanner with the help of the radioactivity it emits as it decays. A PET image can be made based on the distribution and intensity of radioactivity. Therefore, PET imaging allows doctors to visualize where a specific disease target is without surgery.

Existing PET radioligands for amyloid-β bind to the larger plaques but do not bind to the smaller, more toxic aggregates. With the development of new therapies that target the smaller aggregates, it would be beneficial to have a radioligand that can detect these small aggregate forms. This would help determine if a patient will benefit from future treatments and also help evaluate the effectiveness of the treatment.

Antibodies are a part of the body's immune system and identify foreign substances in the body. They have the unique ability to be very selective in binding to specific targets and are a prime option for the development of a more specific PET radioligand compared to the current radioligands.

However, the brain is surrounded by a barrier called the blood-brain barrier (BBB). The BBB is made up of cells that protect the brain by limiting what can cross from the blood into the brain. Antibodies do not cross the BBB well. It is difficult for adequate levels of an antibody to reach the brain to create a

high-contrast PET image. Therefore, a strategy called the "molecular Trojan horse" strategy can be used to carry antibodies into the brain.

The molecular Trojan horse strategy takes advantage of transport proteins, i.e. receptors, on the BBB whose normal function is to transport essential nutrients into the brain from the blood. To take advantage of these receptors, we use a bispecific antibody. This is an antibody that can bind to two targets:

1) the target of interest inside the brain, such as amyloid-β and,
2) one of the receptors on the BBB to ferry the antibody into the brain.

One such receptor is the transferrin receptor (TfR) which carries iron into the brain. TfR has been investigated a lot for transporting new therapies into the brain. A key difference between therapies and PET radioligands is the dose that is used. Therapy doses are substantially higher, sometimes as much as 250x higher, than the doses used for PET imaging with a radioligand.

This thesis focused on evaluating how different binding properties to TfR affect the delivery of antibodies at a low, tracer dose for PET imaging of amyloid-β in the brain.

We started by determining if the molecular Trojan horse strategy for carrying radioligands into the brain would work in a species other than mice. We have previously seen that amyloid-β in mice can be imaged more sensitively with this strategy than with the existing radioligands. In Paper I, we showed that this technique worked in rats as well, suggesting that this strategy could be translated for use for clinical diagnostics in the future.

Affinity is how strongly an antibody binds to its target and is considered an important factor for optimizing brain delivery. There is currently no consensus within the field of how to best measure an antibody's affinity to TfR. In Paper II, we compared four different setups on a Biacore chip and one cell assay for measuring affinity. We found that several assay conditions impact the measured affinity values. Certain conditions on the chip, such as keeping the TfR in a specific orientation, were beneficial for mimicking conditions found in the body.

Affinity has a Goldilocks effect on the brain delivery of therapies: too strong and too weak affinity leads to low brain delivery while a medium-strong affinity is just right. However, it is unclear if this effect changes at the lower doses commonly used for PET imaging. Papers I and III investigated how affinity influences brain delivery at a tracer dose. Stronger affinity to TfR resulted in higher brain levels at a tracer dose suggesting that indeed the effect of affinity on brain delivery is dependent on dose.

Another property of an antibody is how many times it can bind to the target. Antibodies can naturally bind to their target twice but can also be engineered to only bind a single time. Single binding is considered better for brain delivery with the TfR. However, increasing the number of times an antibody binds to its target also increases the affinity. It is currently unclear if the improved brain delivery is caused by the change in the number of binding times or the change in affinity. In Paper IV, we identified a pair of antibodies: one that

binds to TfR once and one that binds twice. These two antibodies had the same affinity. More of the antibody with single binding to TfR entered the brain at a tracer dose than the antibody which bound to TfR twice.

The findings in this thesis suggest that a strong affinity to TfR and binding a single time are likely beneficial properties when harnessing the molecular Trojan horse strategy for delivering PET radioligands to the brain. This will hopefully help develop an antibody-based PET radioligand to image amyloid-β in patients which would aid in a more accurate diagnosis of Alzheimer's disease.

Populärvetenskaplig sammanfattning

Alzheimers sjukdom är den vanligaste formen av demens. Det är en neurodegenerativ sjukdom som karakteriseras av minnesförlust och försämrad kognitiv funktion. Den underliggande orsaken till Alzheimers sjukdom anses vara proteiner som onaturligt klumpar ihop sig för att bilda aggregat: amyloid-β-aggregat ansamlas utanför celler (i form av plack) medan tau aggregerar inne i cellerna. Relativt stora mängder aggregat byggs upp i hjärnan långt innan de karaktäristiska kliniska symtomen uppträder hos patienter. Amyloid-β bildar först små aggregat som sedan fortsätter att klumpa ihop sig till större och större aggregat, för att slutligen bilda plack. De mindre aggregaten anses vara mer toxiska än placken eftersom de orsakar nervcellsdöd i hjärnan. Ju fler små aggregat det finns i hjärnan, desto värre är oftast en patients minnesförlust. Att kunna upptäcka dessa proteiner innan symtom uppträder är viktig för att förbättra chanserna att lyckas med de terapier som för närvarande är tillgängliga för patienter.

En metod som idag används för att diagnostisera Alzheimers sjukdom är positronemissionstomografi (PET). Vid PET-avbildning injiceras en radioaktiv molekyl (även kallad radioligand) i patienten vid en mycket låg dos. Radioliganden kommer att binda till det målsystem som är av intresse hos patienten som undergår PET-undersökningen. Radioaktiviteten som avges från radioliganden sönderfall kan detekteras av PET-scannern. Baserat på radioaktivitetsfördelningen och intensiteten, kan PET-bilder konstrueras. PET-avbildning tillåter läkare att visualisera och kartlägga specifika sjukdomsmål utan operation.

Existerande PET-radioligander för amyloid-β binder till de större placken men inte till de mindre, mer toxiska aggregaten. Med utvecklingen av nya terapier som främst riktar in sig på de mindre aggregaten skulle det vara fördelaktigt att ha en radioligand som kan detektera dessa små aggregatformer. Detta skulle hjälpa till att avgöra om en patient kommer att ha nytta av framtida behandlingar och hjälpa till att utvärdera behandlingens effektivitet.

Antikroppar är en del av kroppens immunförsvar vars uppgift är att identifiera främmande substanser i kroppen. De har den unika förmågan att vara mycket selektiva eftersom de binder till specifika mål och är därför utmärkta alternativ för utveckling av en mer specifik PET-radioligand jämfört med de nuvarande radioliganderna.

Hjärnan är dock omgiven av en cell-baserad barriär som kallas blod-hjärnbarriären (BBB). BBB skyddar hjärnan genom att begränsa vad som kan passera från blod till hjärnan. Antikroppar passar BBB dåligt. Det är därför svårt att få tillräckligt med antikroppsbaserad radioligand att nå hjärnan för att skapa en PET-bild med hög kontrast. En potentiell lösning till detta problem kan vara att använda sig av den så kallade ”molekylära trojanska hästen”-strategin.

Den molekylära trojanska häststrategin utnyttjar transportproteiner, dvs. receptorer, på BBB vars normala funktion är att transportera essentiella substanser in till hjärnan från blodet. För att utnyttja dessa receptorer använder vi en bispecifik antikropp. Det är en antikropp som kan binda till två olika mål:

1. målet av intresse inuti hjärnan, till exempel amyloid-β, och,
2. en av receptorerna på BBB för att transportera antikroppen in till hjärnan.

Ett exempel på en sådan receptor är transferrinreceptorn (TfR) som bär in järn till hjärnan. TfR har undersökts mycket för ändamålet att transportera terapeutiska läkemedel till hjärnan. En viktig skillnad mellan läkemedel ämnade för en terapeutisk effekt och PET-radioligander är dosen som används. Terapidoserna är avsevärt högre, ibland så mycket som 250 gånger högre, än de doser som används för PET-avbildning med en PET-radioligand.

Denna avhandling fokuserade på att utvärdera hur olika bindningsegenskaper till TfR påverkar leveransen av antikroppar till hjärnan vid låga doser för PET-avbildning av amyloid-β i hjärnan.

Vi började med att undersöka om transport av radioligander in till hjärnan med strategin baserad på den molekylära trojanska hästen fungerar i en annan art än möss. Vi har tidigare sett att amyloid-β hos möss kan avbildas mer känsligt med denna strategi, än med de redan existerande PET-radioliganderna. I Artikel I visade vi att denna teknik även fungerade i råttor vilket indikerar att strategin i framtiden skulle kunna användas även för klinisk diagnostik.

Affinitet beskriver hur starkt en antikropp binder till sitt mål och anses vara en viktig faktor för att optimera leverans av antikroppar till hjärnan med TfR. Det finns för nuvarande ingen konsensus inom området för hur man bäst mäter en antikropps affinitet till TfR. I artikel II jämförde vi fyra olika mätinställningar på ett Biacore-chip och en cellanalys för att mäta affiniteten. Vi fann att flera analysförhållanden påverkar de uppmätta affiniteterna. Vissa förhållanden på chipet, t.ex. att arrangera TfR i en specifik orientering, var fördelaktiga för att efterlikna förhållanden som finns i kroppen.

Den optimala affiniteten för TfR-baserad leverans av läkemedel måste vara ”precis lagom”: för stark och för svag affinitet leder till låg hjärnleverans medan en medelstark affinitet är helt rätt. Det är dock oklart om vilken affinitet anses optimalt förändras vid de lägre doserna som vanligtvis används för PET-avbildning. Artiklar I och III undersökte hur affinitet till TfR påverkar leveransen av antikropparna vid en låg dos. Starkare affinitet till TfR resulterade i

högre mängder i hjärnan vid en låg dos, vilket indikerar att effekten är beroende av dosen.

En annan egenskap hos en antikropp är hur många gånger den kan binda till sitt mål. Naturliga antikroppar kan binda till sitt mål två gånger men de kan också konstrueras för att bara binda en endaste gång. En sådan singulär bindning anses vara bättre för transport in till hjärnan med TfR. Antalet gånger en antikropp binder till sitt mål påverkar också affinitet – fler bindningsmöjligheter ger högre affinitet. Det är för närvarande oklart om den förbättrade leveransen till hjärnan orsakas av förändringen i antalet gånger antikroppen binder till sitt mål eller om det är förändringen i affinitet, d.v.s. en lägre affinitet, som ger en ökad transport. I Artikel IV identifierade vi antikropps-par: en som binder till TfR en gång och en som binder två gånger. Dessa två antikroppar hade alltså samma affinitet men olika antal bindningsmöjligheter. Det visade sig att antikroppen med enkel bindning till TfR tog sig in i hjärnan i högre grad vid en låg dos än antikroppen som band till TfR två gånger.

Resultaten i denna avhandling visar att en stark affinitet till TfR och singulär bindning sannolikt är fördelaktiga egenskaper när man utnyttjar den molekylära trojanska häststrategin för att leverera PET-radioligander till hjärnan. Detta arbete kommer förhoppningsvis att hjälpa till att utveckla en antikroppsbaserad PET-radioligand för att avbilda amyloid-β hos patienter vilket skulle hjälpa till med en mer precis diagnos av Alzheimers sjukdom.

Funding

The work presented in this doctoral thesis was performed in the Molecular Geriatrics group at the Department of Public Health and Caring Sciences at Rudbeck Laboratory, Uppsala University, Sweden and at BioArctic AB, Sweden. The molecular imaging work was performed at the SciLifeLab Pilot Facility for Preclinical PET-MRI, a Swedish nationally available imaging platform at Uppsala University, Sweden, financed by the Knut and Alice Wallenberg Foundation. This project has received funding from the European Union's Horizon 2020 and innovation programme under the Marie Skłodowska-Curie grant agreement No 813528. I would also like to thank the funding bodies for financial support and travel grants over the years, including: the Swedish Research Council, the Swedish Innovation Agency, Alzheimerfonden, Hjärnfonden, Hedlunds stiftelse, Torsten Söderbergs stiftelse, Åhlénstifelsen, Magnus Bergvalls stiftelse, Konung Gustaf V:s och Drottning Victorias frimuarestiftelse, Åke Wibergs stiftelse, Stiftelsen för gamla tjänarinnor, Stohnes stiftelse, and Anna Maria Lundins scholarship (Smålands nation).

Schematic images were created by the author in part using BioRender.

Acknowledgements

As my PhD comes to an end, I am reminded of a quote from Winnie-the-Pooh that reflects my feelings exactly:

"How lucky am I to have something that makes saying goodbye so hard"
– A.A. Milne

These last few years have had their ups and downs but I am immensely grateful to the amazing community that has supported me and for the many new friends I have made along the way.

I would like to start with thanking my supervisors for making this PhD an enjoyable experience. I feel very lucky indeed to have had such great mentors. You each brought your own, unique wisdom and experiences in a way that complimented each other wonderfully. I know I am the scientist I am today because of all of you.

Stina, thank you for having my back from the very beginning. You are an inspiring scientist and group leader. Thank you for making the intense *in vivo* experimental days more fun. I will remember our jacuzzi chats in Colorado fondly.

Thank you **Johanna** for your unwavering support. I very much enjoyed our 1:1 meetings and your passion for science is very motivating. No matter what idea I had, you were always ready to brainstorm further. I knew I could count on you which was very reassuring.

I am so grateful **Dag** that we got to share our first GRC experience together. Your enthusiasm in scientific discussions is very contagious. Your encouragement and assistance helped me endure the struggles of the rat paper and the night at the PPP with you and Stina, scanning rats and watching football, is a special memory from the last few years.

Thank you **Ken**, for taking me under your wing and teaching me everything about proteins. I remember how excited I was when you asked if I would like you to be my supervisor and I have never once regretted saying yes. Thank

you for keeping me active with your Tabata classes and sharing your home-brewed beers with me – hopefully I can try my hand at the apple milkshake beer soon.

Sahar, although we were not in the lab in Uppsala very often at the same time, I knew you were available should I need extra help or someone to turn to. Thank you for bringing extra sweetness to the lunch and fika conversations.

To the MolGer lab in Uppsala, thank you for being so friendly and welcoming from Day 1. While trying to decide between living in Stockholm or Uppsala, Stina recommended starting in Uppsala because the students hang out together in their free time. She was definitely correct. These last few years have been filled with many AWs, fantastic memories, and laughs ☺

Thank you to my fellow triplets: **Eva** and **Mengfei**. We started this journey together and over the past years, you have both become very special to me. Thank you both for all of your support. I have shared cherished memories with each of you. Thank you, **Eva**, for our long chats and all of our road trip adventures, especially our trip to the towns along Vättern. You inspire me to explore Sweden more. **Mengfei**, you are a kind-hearted, caring friend, and one of the hardest workers I know. Thank you for joining for "swim and fika", for the home-made dumpling night and for introducing me to hot pot!

Tobias M, BabyT, I have very much enjoyed sharing an office with you and our countless conversations. Thank you for the viewings of "The Boys" and the fikas with **Sofia**! **Chiara**, thank you for including me in your book club and for introducing me to the Baci chocolate spread. To the newest MolGer PhDs: **Amelia**, you are the game master of the group and bring an unmatched, positive energy to lab. Thank you, **Abdul**, for teaching me western blot and celebrating the little victories. Your smile brightens up the lab. And **Elin**, you are a lovely friend and a great motivator for swimming! I wish the three of you the very best with your PhD journeys! Thank you, **Tiffany**, for becoming such a dear friend in such a short time. You are a sweetheart and it's been an absolute delight getting to know you both in and outside the lab. And thank you so much for the very thorough proofreading. **Khalid**, you are so sincere. Thank you for the pleasant chats.

Ximena, your organization and hard work keeps the lab running smoothly. Thank you for always helping me find all the supplies I needed. Tack, **Vilmantas** and **Anna**, for the lovely conversations and fun anecdotes at fika. **Wojciech**, thank you for sharing photos of Oatley. Best of luck with your growing lab section! Thank you, **Sara**, for your help with all things radiochemistry-related. It was very fun getting to know you during the consortium meetings and even more so now that you have moved to Uppsala.

Jinar, you are a ray of sunshine and I always feel happier after chatting with you. Your love for anything Canadian is so cute and your drive to continue with Med school after a PhD, inspiring. **Emma**, you are so thoughtful, strong, and sweet. Thank you to both you and **Robin** for helping me get breaks from the stresses of PhD life and to **Saga** and **Alfred** for always putting a smile on my face ☺. **Rebecca**, I very much enjoyed collaborating with you. Thank you for teaching me capillary depletion and for the friendly company while working in the lab together. Thank you, **Silvio**, **Tobias G**, and **Anish**, for the fun conversations at lunch and the AWs. The lab has definitely not been the same since you guys left. **Tobias G**, I hope your research has continued to bear fruit! **Maria** and **Evangelos**, sharing an office with you for the first few months was very fun and I am grateful that we can continue being colleagues at BioArctic.

Agnieszka, thank you for being a dedicated swim buddy and for becoming such a close friend. I loved taking Swedish classes with you and I hope we can continue our "practice Swedish" fikas (with maybe some more actual Swedish). **Ulrika**, thank you for joining for "swim and fika"! You always pushed us to swim further and longer and it's not the same without you there.

Finally, a heartfelt thank you to past and current MolGer members, including **Martin I**, **Joakim**, **Johanna R**, **Linn**, **Sara EL**, **Agata**, **Lara**, **Sergey**, **Elnaz**, **Sona**, and **Elena**, for the warm smiles, friendly company and scientific support over the years.

Thank you also to **Jonas** for teaching us Marie Curie triplets radiochemistry. Hope to see you (and Stina) at Fyrishov again soon!

Tack så jättemycket till allihopa på BioArctic, speciallt **Gunilla O** och **Lars**, för att ni välkomnade mig till BioArctic-famijlen. Thank you to all past and present BioArctic employees for the fun memories over the years and helping me practice my Swedish. An extra thank you to the members of the science sections for your support and amiable company in the lab and the many, many fika breaks. It has been a pleasure working alongside all of you and I am excited to continue in the autumn.

Thank you, **Olof**, for offering me this once-in-a-lifetime opportunity. I will never forget my surprise when I asked for 5 weeks unpaid leave for my trip to Nepal and you told me that my vacation days in Sweden would cover it!

To **Biljana**, thank you for welcoming me into the section and for our lovely 1:1 chats.

Tack **Peo** for the insightful scientific discussions. Your knowledge of TfR and the BBB is truly impressive. Thank you, **Martin** and **Sofia**, for all of the great

conversations about my *in vivo* data and life in general. Thank you to **Lisa** and **Josephine** for teaching me about and helping me with transfections and protein production. **Sunitha**, thank you very much for all of your help with the cell experiments. It has been so fun working with you in the cell lab.

Thank you **Patrik** for teaching me all about the Biacore and answering my countless questions. I have thoroughly enjoyed reading Swedish children's books with you and I hope that now, we will finally be able to finish Nalle Puh! Thank you **Ronny** for showing me the ropes when I first started at BioArctic. Together with **Jessica** and **Alex**, you were very fun office mates. I am grateful that I could share my lab struggles and victories over these last few years with you.

Thank you **Christer**, for your help with all of the publication approvals over the last few years. I know I didn't always give you the most time to get it all sorted but you always pulled through for me in the end. **Else-Britt**, thank you for all of your help booking flights and accommodation for conferences. Without your organisational skills, my travels would definitely not have gone as smoothly. Tack, **Gunilla A**, for helping me with my visa extension application and for organizing the very helpful Swedish conversation course. **Jan**, thank you for helping me navigate the Swedish financial system. Thank you, **Mats**, for all of your IT support.

Thank you very much to the Marie Curie PET-AlphaSY consortium for providing this unique opportunity. Thank you **Matthias Herth**, **Ulla Kløve Jakobsen**, and all of the supervisors and fellow PhD students for making the consortium meetings both educational and fun.

Thank you to my co-authors in Turku, **Francisco** and **Merja**, for making Paper I possible.

I am also very grateful to the friends I have met outside of the lab. Thank you, **Peter** and **Sandra**, for adopting a Canadian. Not only did you make my first Christmas away from home incredibly special, but all our board game nights, brunches, summer dips in the river/lakes, and adventures have left me with many cherished memories.

Nataša, thank you for our many brunches and excursions in Stockholm. I love trying new brunch spots with you. I'm grateful we could stay in touch when you moved to France but extra (although slightly selfishly) grateful to have you back in Sweden. Tack **Katrín** for encouraging me to dance Bachata. I hope we can go canoeing again soon. **Viktoria**, you are a great singer and skilled event planner. Your parties are very entertaining and I always enjoy catching up with you.

I would also like to thank my friends who live around the world for their enormous support. **Katie**, **Ivette**, **Melina**, **Annika**, and **Emma**, I am so grateful that we have managed to stay connected with regular skype chats and in person visits despite Covid and the 1000s of kilometres between us.

And finally, to my family: **Mom**, **Dad**, **Stephanie**, and **Aman**. Thank you for always being here for me, even from the other side of the ocean. Despite the distance, I always knew I could count on you – for proofreading, explaining the chemistry behind my purification techniques, labelling 1224 Eppendorf tubes, helping to figure out my image analysis, listening when things were tough, and celebrating the big and little things. I love you soooooo much and can't imagine having done this without you.

References

1. Dementia. *World Health Organization* (2023). Available at: https://www.who.int/news-room/fact-sheets/detail/dementia. (Accessed: 5th July 2023)
2. Monteiro, A. R., Barbosa, D. J., Remião, F. & Silva, R. Alzheimer's disease: Insights and new prospects in disease pathophysiology, biomarkers and disease-modifying drugs. *Biochem. Pharmacol.* **211**, (2023).
3. Yang, H. D., Kim, D. H., Lee, S. B. & Young, L. D. History of Alzheimer's Disease. *Dement. Neurocognitive Disord.* **15**, 115–121 (2016).
4. Glenner, G. G. & Wong, C. W. Alzheimer's disease: Initial report of the purification and characterization of a novel cerebrovascular amyloid protein. *Biochem. Biophys. Res. Commun.* **120**, 885–890 (1984).
5. Tanzi, R. E. *et al.* Amyloid β Protein Gene: cDNA, mRNA Ditibuton, and Genetic Lie Near the Alzheimer Locus. *Science (80-.).* **235**, (1987).
6. Goedert, M., Wischik, C. M., Crowther, R. A., Walker, J. E. & Klug, A. Cloning and sequencing of the cDNA encoding a core protein of the paired helical filament of Alzheimer disease: Identification as the microtubule-associated protein tau. *Proc. Natl. Acad. Sci. U. S. A.* **85**, 4051–4055 (1988).
7. Lee, V. M. Y., Balin, B. J., Otvos, L. & Trojanowski, J. Q. A68: A major subunit of paired helical filaments and derivatized forms of normal tau. *Science (80-.).* **251**, 675–678 (1991).
8. Dubois, B. *et al. Preclinical Alzheimer's disease: Definition, natural history, and diagnostic criteria*. *Alzheimer's and Dementia* **12**, (2016).
9. Bertram, L. & Tanzi, R. E. The genetic epidemiology of neurodegenerative disease. *J. Clin. Invest.* **115**, 1449–1457 (2005).
10. van der Lee, S. J. *et al.* The effect of APOE and other common genetic variants on the onset of Alzheimer's disease and dementia: a community-based cohort study. *Lancet Neurol.* **17**, 434–444 (2018).
11. Mullan, M. *et al.* A pathogenic mutation for probable Alzheimer's disease in the APP gene at the N-terminus of β-amyloid. *Nat. Genet.* **1**, 345–347 (1992).
12. Nilsberth, C. *et al.* The 'Arctic' APP mutation (E693G) causes Alzheimer's disease by enhanced Aβ protofibril formation. *Nat. Neurosci.* **4**, 887–893 (2001).
13. Bi, C., Bi, S. & Li, B. Processing of mutant β-amyloid precursor protein and the clinicopathological features of familial alzheimer's disease. *Aging Dis.* **10**, 383–403 (2019).
14. Pagnon De la Vega, M. *et al.* The Uppsala APP deletion causes early onset autosomal dominant Alzheimer's disease by altering APP processing and increasing amyloid β fibril formation. *Sci. Transl. Med.* **13**, (2021).

15. Kent, S. A., Spires-Jones, T. L. & Durrant, C. S. *The physiological roles of tau and Aβ: implications for Alzheimer's disease pathology and therapeutics*. *Acta Neuropathologica* **140**, (Springer Berlin Heidelberg, 2020).
16. Walsh, D. M., Lomakin, A., Benedek, G. B., Condron, M. M. & Teplow, D. B. Amyloid β-protein fibrillogenesis: Detection of a protofibrillar intermediate. *J. Biol. Chem.* **272**, 22364–22372 (1997).
17. Hardy, J. & Higgins, G. Alzheimer' s Disease: The Amyloid Cascade Hypothesis. *Science (80-.).* **256**, 184–185 (1992).
18. McLean, C. A. *et al.* Soluble pool of Aβ amyloid as a determinant of severity of neurodegeneration in Alzheimer's disease. *Ann. Neurol.* **46**, 860–866 (1999).
19. Näslund, J. *et al.* Correlation between elevated levels of amyloid β-peptide in the brain and cognitive decline. *J. Am. Med. Assoc.* **283**, 1571–1577 (2000).
20. Esparza, T. J. *et al.* Amyloid-beta oligomerization in Alzheimer dementia versus high-pathology controls. *Ann. Neurol.* **73**, 104–119 (2013).
21. Lambert, M. P. *et al.* Diffusible, nonfibrillar ligands derived from Aβ1–42 are potent central nervous system neurotoxins. *Proc. Natl. Acad. Sci. U. S. A.* **95**, 6448–6453 (1998).
22. Hartley, D. M. *et al.* Protofibrillar intermediates of amyloid β-protein induce acute electrophysiological changes and progressive neurotoxicity in cortical neurons. *J. Neurosci.* **19**, 8876–8884 (1999).
23. Söllvander, S. *et al.* Accumulation of amyloid-β by astrocytes result in enlarged endosomes and microvesicle-induced apoptosis of neurons. *Mol. Neurodegener.* **11**, 1–19 (2016).
24. Konstantinidis, E. *et al.* Intracellular deposits of amyloid-beta influence the ability of human iPSC-derived astrocytes to support neuronal function. *J. Neuroinflammation* **20**, 1–17 (2023).
25. Selkoe, D. J. & Hardy, J. The amyloid hypothesis of Alzheimer's disease at 25 years. *EMBO Mol. Med.* **8**, 595–608 (2016).
26. Hillen, H. The Beta Amyloid Dysfunction (BAD) Hypothesis for Alzheimer's Disease. *Front. Neurosci.* **13**, 1–10 (2019).
27. Sasaguri, H. *et al.* APP mouse models for Alzheimer's disease preclinical studies. *EMBO J.* **36**, 2473–2487 (2017).
28. Jack, C. R. *et al.* Hypothetical Pathological Cascade in Alheimer's Disease. *Lancet Neurol.* **9**, 1–20 (2010).
29. Cummings, J. *et al.* Aducanumab produced a clinically meaningful benefit in association with amyloid lowering. *Alzheimer's Res. Ther.* **13**, 10–12 (2021).
30. van Dyck, C. H. *et al.* Lecanemab in early Alzheimer's Disease. *N. Engl. J. Med.* **388**, 9–21 (2023).
31. Arndt, J. W. *et al.* Structural and kinetic basis for the selectivity of aducanumab for aggregated forms of amyloid-β. *Sci. Rep.* **8**, 1–16 (2018).
32. Sevigny, J. *et al.* The antibody aducanumab reduces Aβ plaques in Alzheimer's disease. *Nature* **537**, 50–56 (2016).
33. Dunn, B., Stein, P. & Cavazzoni, P. Approval of Aducanumab for Alzheimer Disease — the FDA's Perspective. *JAMA Intern. Med.* **181**, 1276–1278 (2021).

34. Fleck, L. M. Alzheimer's and Aducanumab: Unjust Profits and False Hopes. *Hastings Cent. Rep.* **51**, 9–11 (2021).
35. Mullard, A. Landmark Alzheimer's drug approval confounds research community. *Nature* **594**, 309–310 (2021).
36. FDA Grants Accelerated Approval for Alzheimer's Disease Treatment. *FDA News Release* (2023). Available at: https://www.fda.gov/news-events/press-announcements/fda-grants-accelerated-approval-alzheimers-disease-treatment. (Accessed: 5th July 2023)
37. FDA Converts Novel Alzheimer's Disease Treatment to Traditional Approval. *FDA News Release* (2023). Available at: https://www.fda.gov/news-events/press-announcements/fda-converts-novel-alzheimers-disease-treatment-traditional-approval. (Accessed: 7th July 2023)
38. Englund, H. *et al.* Sensitive ELISA detection of amyloid-β protofibrils in biological samples. *J. Neurochem.* **103**, 334–345 (2007).
39. Söderberg, L. *et al.* Lecanemab, Aducanumab, and Gantenerumab — Binding Profiles to Different Forms of Amyloid-Beta Might Explain Efficacy and Side Effects in Clinical Trials for Alzheimer's Disease. *Neurotherapeutics* **20**, 195–206 (2023).
40. DeMattos, R. B. *et al.* A Plaque-Specific Antibody Clears Existing β-amyloid Plaques in Alzheimer's Disease Mice. *Neuron* **76**, 908–920 (2012).
41. Michno, W. *et al.* Pyroglutamation of amyloid-βx-42 (Aβx-42) followed by Aβ1-40 deposition underlies plaque polymorphism in progressing Alzheimer's disease pathology. *J. Biol. Chem.* **294**, 6719–6732 (2019).
42. D'Arrigo, C., Tabaton, M. & Perico, A. N-terminal truncated pyroglutamyl β amyloid peptide Aβpy3-42 shows a faster ggregation kinetics than the full-length Aβ1-42. *Biopolymers* **91**, 861–873 (2009).
43. Sims, J. R. *et al.* Donanemab in Early Symptomatic Alzheimer Disease: The TRAILBLAZER-ALZ 2 Randomized Clinical Trial. *Jama* **46285**, 1–16 (2023).
44. Bohrmann, B. *et al.* Gantenerumab: A novel human anti-Aβ antibody demonstrates sustained cerebral amyloid-β binding and elicits cell-mediated removal of human amyloid-β. *J. Alzheimer's Dis.* **28**, 49–69 (2012).
45. Bateman, R. J. *et al.* Gantenerumab: an anti-amyloid monoclonal antibody with potential disease-modifying effects in early Alzheimer's disease. *Alzheimer's Res. Ther.* **14**, 1–17 (2022).
46. Niewoehner, J. *et al.* Increased Brain Penetration and Potency of a Therapeutic Antibody Using a Monovalent Molecular Shuttle. *Neuron* **81**, 49–60 (2014).
47. Weber, F. *et al.* Brain Shuttle Antibody for Alzheimer's Disease with Attenuated Peripheral Effector Function due to an Inverted Binding Mode. *Cell Rep.* **22**, 149–162 (2018).
48. Ossenkoppele, R. *et al.* Prevalence of amyloid PET positivity in dementia syndromes: a meta-analysis. *JAMA* **313**, 1939–1949 (2015).
49. Dupont, A. C., Largeau, B., Guilloteau, D., Santiago Ribeiro, M. J. & Arlicot, N. The Place of PET to Assess New Therapeutic Effectiveness in Neurodegenerative Diseases. *Contrast Media Mol. Imaging* **Article ID**, 1–15 (2018).

50. Alexander, G. E., Chen, K., Pietrini, P., Rapoport, S. I. & Reiman, E. M. Longitudinal PET evaluation of cerebral metabolic decline in dementia: A potential outcome measure in Alzheimer's disease treatment studies. *Am. J. Psychiatry* **159**, 738–745 (2002).
51. Klunk, W. E. *et al.* Imaging Brain Amyloid in Alzheimer's Disease with Pittsburgh Compound-B. *Ann. Neurol.* **55**, 306–319 (2004).
52. Sehlin, D. & Syvänen, S. Engineered antibodies: new possibilities for brain PET ? *Eur. J. Nucl. Med. Mol. Imaging* **11**, 1–11 (2019).
53. Abrahamson, E. E. *et al.* 11C-PiB PET can underestimate brain amyloid-β burden when cotton wool plaques are numerous. *Brain* **145**, 2161–2176 (2022).
54. Schöll, M. *et al.* Low PiB PET retention in presence of pathologic CSF biomarkers in Arctic APP mutation carriers. *Neurology* **79**, 229–236 (2012).
55. Robinson, J. L. *et al.* Neurodegenerative disease concomitant proteinopathies are prevalent, age-related and APOE4-associated. *Brain* **141**, 2181–2193 (2018).
56. Karanth, S. *et al.* Prevalence and Clinical Phenotype of Quadruple Misfolded Proteins in Older Adults. *JAMA Neurol.* **77**, 1299–1307 (2020).
57. Dijkers, E. C. *et al.* Biodistribution of 89 Zr-trastuzumab and PET Imaging of HER2-Positive Lesions in Patients with Metastatic Breast Cancer. *Clin. Pharmacol. Ther.* **87**, 586–592 (2010).
58. van Dongen, G. A. M. S., Poot, A. J. & Vugts, D. J. PET imaging with radiolabeled antibodies and tyrosine kinase inhibitors: Immuno-PET and TKI-PET. *Tumor Biol.* **33**, 607–615 (2012).
59. Wei, W. *et al.* ImmunoPET: Concept, Design, and Applications. *Chem. Rev.* **120**, 3787–3851 (2020).
60. Magnusson, K. *et al.* Specific uptake of an amyloid-β protofibril-binding antibody-tracer in AβPP transgenic mouse brain. *J. Alzheimer's Dis.* **37**, 29–40 (2013).
61. Hultqvist, G., Syvänen, S., Fang, X. T., Lannfelt, L. & Sehlin, D. Bivalent brain shuttle increases antibody uptake by monovalent binding to the transferrin receptor. *Theranostics* **7**, 308–318 (2017).
62. Syvänen, S. *et al.* Efficient clearance of Aβ protofibrils in AβPP-transgenic mice treated with a brain-penetrating bifunctional antibody. *Alzheimer's Res. Ther.* **10**, 1–10 (2018).
63. Sehlin, D. *et al.* Brain delivery of biologics using a cross-species reactive transferrin receptor 1 VNAR shuttle. *FASEB J.* **34**, 13272–13283 (2020).
64. Johnsen, K. B., Burkhart, A., Thomsen, L. B., Andresen, T. L. & Moos, T. Targeting the transferrin receptor for brain drug delivery. *Prog. Neurobiol.* **181**, 1–30 (2019).
65. Sweeney, M. D., Zhao, Z., Montagne, A., Nelson, A. R. & Zlokovic, B. V. Blood-brain barrier: From physiology to disease and back. *Physiol. Rev.* **99**, 21–78 (2019).
66. Azarmi, M., Maleki, H., Nikkam, N. & Malekinejad, H. Transcellular brain drug delivery: A review on recent advancements. *Int. J. Pharm.* **586**, 1–15 (2020).

67. Chowdhury, E. A. *et al.* Understanding the brain uptake and permeability of small molecules through the BBB: A technical overview. *J. Cereb. Blood Flow Metab.* **41**, 1797–1820 (2021).
68. Andjelkovic, A. V. *et al.* Blood-Brain Barrier Dysfunction in Normal Aging and Neurodegeneration: Mechanisms, Impact, and Treatments. *Stroke* **54**, 661–672 (2023).
69. Stamatovic, S. M., Johnson, A. M., Keep, R. F. & Andjelkovic, A. V. Junctional proteins of the blood-brain barrier: New insights into function and dysfunction. *Tissue Barriers* **4**, 1–12 (2016).
70. Kutuzov, N., Flyvbjerg, H. & Lauritzen, M. Contributions of the glycocalyx, endothelium, and extravascular compartment to the blood–brain barrier. *Proc. Natl. Acad. Sci. U. S. A.* **115**, E9429–E9438 (2018).
71. Armulik, A. *et al.* Pericytes regulate the blood-brain barrier. *Nature* **468**, 557–561 (2010).
72. Villasenõr, R. *et al.* Trafficking of Endogenous Immunoglobulins by Endothelial Cells at the Blood-Brain Barrier. *Sci. Rep.* **6**, 1–10 (2016).
73. Kaplan, L., Chow, B. W. & Gu, C. Neuronal regulation of the blood–brain barrier and neurovascular coupling. *Nat. Rev. Neurosci.* **21**, 416–432 (2020).
74. Syvänen, S., Edén, D. & Sehlin, D. Cationization increases brain distribution of an amyloid-beta protofibril selective F(ab')2 fragment. *Biochem. Biophys. Res. Commun.* **493**, 120–125 (2017).
75. Finch, A. & Pillans, P. P-glycoprotein and its role in drug-drug interactions. *Aust. Prescr.* **37**, 137–139 (2014).
76. Stanimirovic, D. B., Sandhu, J. K. & Costain, W. J. Emerging Technologies for Delivery of Biotherapeutics and Gene Therapy Across the Blood–Brain Barrier. *BioDrugs* **32**, 547–559 (2018).
77. Zhao, Z. & Zlokovic, B. V. Therapeutic TVs for Crossing Barriers in the Brain. *Cell* **182**, 267–269 (2020).
78. Zuchero, Y. J. Y. *et al.* Discovery of Novel Blood-Brain Barrier Targets to Enhance Brain Uptake of Therapeutic Antibodies. *Neuron* **89**, 70–82 (2016).
79. Edavettal, S. *et al.* Enhanced delivery of antibodies across the blood-brain barrier via TEMs with inherent receptor-mediated phagocytosis. *Med* **3**, 860–882 (2022).
80. Pornnoppadol, G. *et al.* Bispecific antibody shuttles targeting CD98hc mediate efficient and long-lived brain delivery of IgGs. *bioRxiv* 2023.04.29.538811 (2023). doi:10.1101/2023.04.29.538811
81. Boado, R. J. *et al.* Genetic engineering of a lysosomal enzyme fusion protein for targeted delivery across the human blood-brain barrier. *Biotechnol. Bioeng.* **99**, 475–484 (2008).
82. Boado, R. J., Hui, E. K. W., Lu, J. Z., Sumbria, R. K. & Pardridge, W. M. Blood-brain barrier molecular trojan horse enables imaging of brain uptake of radioiodinated recombinant protein in the rhesus monkey. *Bioconjug. Chem.* **24**, 1741–1749 (2013).
83. Boado, R. J. & Pardridge, W. M. Brain and organ uptake in the Rhesus monkey in vivo of recombinant iduronidase compared to an insulin receptor antibody-iduronidase fusion protein. *Mol. Pharm.* **14**, 1271–1277 (2017).

84. Morito, T. *et al.* Synthesis and pharmacokinetic characterisation of a fluorine-18 labelled brain shuttle peptide fusion dimeric affibody. *Sci. Rep.* **11**, 1–12 (2021).
85. Tian, X. *et al.* On the shuttling across the blood-brain barrier via tubule formation: Mechanism and cargo avidity bias. *Sci. Adv.* **6**, 1–16 (2020).
86. Kawabata, H. *et al.* Molecular cloning of transferrin receptor 2: A new member of the transferrin receptor-like family. *J. Biol. Chem.* **274**, 20826–20832 (1999).
87. Deaglio, S. *et al.* Structural, functional, and tissue distribution analysis of human transferrin receptor-2 by murine monoclonal antibodies and a polyclonal antiserum. *Blood* **100**, 3782–3789 (2002).
88. West, A. P. *et al.* Comparison of the interactions of transferrin receptor and transferrin receptor 2 with transferrin and the hereditary hemochromatosis protein HFE. *J. Biol. Chem.* **275**, 38135–38138 (2000).
89. Kleven, M. D., Jue, S. & Enns, C. A. Transferrin Receptors TfR1 and TfR2 Bind Transferrin through Differing Mechanisms. *Biochemistry* **57**, 1552–1559 (2018).
90. Lawrence, C. M. *et al.* Crystal structure of the ectodomain of human transferrin receptor. *Science (80-.).* **286**, 779–782 (1999).
91. Cheng, Y. *et al.* Structure of the Human Transferrin Receptor-Transferrin Complex Albert Einstein College of Medicine. *Cell* **116**, 565–576 (2004).
92. Bateman, A. *et al.* UniProt: The universal protein knowledgebase in 2021. *Nucleic Acids Res.* **49**, D480–D489 (2021).
93. Zhang, W. *et al.* Differential expression of receptors mediating receptor-mediated transcytosis (RMT) in brain microvessels, brain parenchyma and peripheral tissues of the mouse and the human. *Fluids Barriers CNS* **17**, 1–30 (2020).
94. Montemiglio, L. C. *et al.* Cryo-EM structure of the human ferritin–transferrin receptor 1 complex. *Nat. Commun.* **10**, 1–8 (2019).
95. Aisen, P., Leibman, A. & Zweier, J. Stoichiometric and site characteristics of the binding of iron to human transferrin. *J. Biol. Chem.* **253**, 1930–1937 (1978).
96. Kretchmar, S. A., Teixeira, M., Huynh, B. & Raymond, K. N. Mössbauer studies of electrophoretically purified monoferric and diferric human transferrin. *Biol. Met.* **1**, 26–32 (1988).
97. Cheng, Y., Zak, O., Aisen, P., Harrison, S. C. & Walz, T. Single particle reconstruction of the human apo-transferrin-transferrin receptor complex. *J. Struct. Biol.* **152**, 204–210 (2005).
98. Eckenroth, B. E., Steere, A. N., Chasteen, N. D., Everse, S. J. & Mason, A. B. How the binding of human transferrin primes the transferrin receptor potentiating iron release at endosomal pH. *Proc. Natl. Acad. Sci. U. S. A.* **108**, 13089–13094 (2011).
99. Giannetti, A. M., Snow, P. M., Zak, O. & Björkman, P. J. Mechanism for multiple ligand recognition by the human transferrin receptor. *PLoS Biol.* **1**, 341–350 (2003).

100. Villaseñor, R., Schilling, M., Sundaresan, J., Lutz, Y. & Collin, L. Sorting Tubules Regulate Blood-Brain Barrier Transcytosis. *Cell Rep.* **21**, 3256–3270 (2017).
101. Burkhart, A. *et al.* Expression of Iron-Related Proteins at the Neurovascular Unit Supports Reduction and Reoxidation of Iron for Transport Through the Blood-Brain Barrier. *Mol. Neurobiol.* **53**, 7237–7253 (2016).
102. Mayle, K. M., Le, A. M. & Kamei, D. T. The intracellular trafficking pathway of transferrin. *Biochim. Biophys. Acta - Gen. Subj.* **1820**, 264–281 (2012).
103. Li, L. *et al.* Binding and uptake of H-ferritin are mediated by human transferrin receptor-1. *Proc. Natl. Acad. Sci. U. S. A.* **107**, 3505–3510 (2010).
104. Moody, P. R. *et al.* Receptor Crosslinking: A General Method to Trigger Internalization and Lysosomal Targeting of Therapeutic Receptor:Ligand Complexes. *Mol. Ther.* **23**, 1888–1898 (2015).
105. Boado, R. J., Zhou, Q. H., Lu, J. Z., Hui, E. K. W. & Pardridge, W. M. Pharmacokinetics and brain uptake of a genetically engineered bifunctional fusion antibody targeting the mouse transferrin receptor. *Mol. Pharm.* **7**, 237–244 (2010).
106. Yu, Y. J. *et al.* Boosting brain uptake of a therapeutic antibody by reducing its affinity for a transcytosis target. *Sci. Transl. Med.* **3**, 1–9 (2011).
107. Webster, C. I. *et al.* Enhanced delivery of IL-1 receptor antagonist to the central nervous system as a novel anti-Transferrin receptor-IL-1RA fusion reverses neuropathic mechanical hypersensitivity. *Pain* **158**, 660–668 (2017).
108. Rofo, F. *et al.* Enhanced neprilysin-mediated degradation of hippocampal Aβ42 with a somatostatin peptide that enters the brain. *Theranostics* **11**, 789–804 (2021).
109. Rofo, F. *et al.* A Brain-Targeting Bispecific-Multivalent Antibody Clears Soluble Amyloid-Beta Aggregates in Alzheimer's Disease Mice. *Neurotherapeutics* **19**, 1588–1602 (2022).
110. Rofo, F. *et al.* Blood–brain barrier penetrating neprilysin degrades monomeric amyloid-beta in a mouse model of Alzheimer's disease. *Alzheimer's Res. Ther.* **14**, 1–19 (2022).
111. Roshanbin, S. *et al.* Reduction of αSYN Pathology in a Mouse Model of PD Using a Brain-Penetrating Bispecific Antibody. *Pharmaceutics* **14**, 1–16 (2022).
112. Su, S., Esparza, T. J. & Brody, D. L. *Selection of single domain anti-transferrin receptor antibodies for blood-brain barrier transcytosis using a neurotensin based assay and histological assessment of target engagement in a mouse model of Alzheimer's related amyloid-beta pathology*. *PLoS ONE* **17**, (2022).
113. Friden, P. M. *et al.* Anti-transferrin receptor antibody and antibody-drug conjugates cross the blood-brain barrier. *Proc. Natl. Acad. Sci. U. S. A.* **88**, 4771–4775 (1991).
114. Wu, D. & Pardridge, W. M. Neuroprotection with noninvasive neurotrophin delivery to the brain. *Proc. Natl. Acad. Sci. U. S. A.* **96**, 254–259 (1999).
115. Thom, G. *et al.* Enhanced Delivery of Galanin Conjugates to the Brain through Bioengineering of the Anti-Transferrin Receptor Antibody OX26. *Mol. Pharm.* **15**, 1420–1431 (2018).

116. Campos, C. R., Kemble, A. M., Niewoehner, J., Freskgård, P. O. & Urich, E. Brain Shuttle Neprilysin reduces central Amyloid-β levels. *PLoS One* **15**, 1–12 (2020).
117. Yu, Y. J. *et al.* Therapeutic bispecific antibodies cross the blood-brain barrier in nonhuman primates. *Sci. Transl. Med.* **6**, 1–11 (2014).
118. Sonoda, H. *et al.* A Blood-Brain-Barrier-Penetrating Anti-human Transferrin Receptor Antibody Fusion Protein for Neuronopathic Mucopolysaccharidosis II. *Mol. Ther.* **26**, 1366–1374 (2018).
119. Kariolis, M. S. *et al.* Brain delivery of therapeutic proteins using an Fc fragment blood-brain barrier transport vehicle in mice and monkeys. *Sci. Transl. Med.* **12**, (2020).
120. Okuyama, T. *et al.* Iduronate-2-Sulfatase with Anti-human Transferrin Receptor Antibody for Neuropathic Mucopolysaccharidosis II: A Phase 1/2 Trial. *Mol. Ther.* **27**, 456–464 (2019).
121. Giugliani, R. *et al.* Iduronate-2-sulfatase fused with anti-hTfR antibody, pabinafusp alfa, for MPS-II: A phase 2 trial in Brazil. *Mol. Ther.* **29**, 2378–2386 (2021).
122. Okuyama, T. *et al.* A Phase 2/3 Trial of Pabinafusp Alfa, IDS Fused with Anti-Human Transferrin Receptor Antibody, Targeting Neurodegeneration in MPS-II. *Mol. Ther.* **29**, 671–679 (2021).
123. Terstappen, G. C., Meyer, A. H., Bell, R. D. & Zhang, W. Strategies for delivering therapeutics across the blood–brain barrier. *Nat. Rev. Drug Discov.* **20**, 362–383 (2021).
124. Mullard, A. Blood–brain barrier-traversing biologic secures regulatory approval, in Japan. *Nature Reviews Drug Discovery* **20**, 332 (2021).
125. Ullman, J. C. *et al.* Brain delivery and activity of a lysosomal enzyme using a blood-brain barrier transport vehicle in mice. *Sci. Transl. Med.* **12**, 1–13 (2020).
126. Arguello, A. *et al.* Iduronate-2-sulfatase transport vehicle rescues behavioral and skeletal phenotypes in a mouse model of Hunter syndrome. *JCI Insight* **6**, 1–16 (2021).
127. Denali Therapeutics Announces New Interim Data from DNL310 Phase 1 / 2 Study for MPS II and DNL126 Preclinical Data for MPS IIIA at. *Denali Therapeutics Inc.* (2023). Available at: https://www.globenewswire.com/news-release/2023/02/22/2613774/0/en/Denali-Therapeutics-Announces-New-Interim-Data-from-DNL310-Phase-1-2-Study-for-MPS-II-and-DNL126-Preclinical-Data-for-MPS-IIIA-at-WORLDSymposium.html. (Accessed: 17th July 2023)
128. Logan, T. *et al.* Rescue of a lysosomal storage disorder caused by Grn loss of function with a brain penetrant progranulin biologic. *Cell* **184**, 4651-4668.e25 (2021).
129. Reich, A. M. *et al.* Rescue of FTLD-associated TDP-43 pathology and neurodegeneration by peripheral AAV-mediated expression of brain-penetrant progranulin. *bioRxiv* 2023.07.14.549089 (2023). doi:10.1101/2023.07.14.549089

130. van Lengerich, B. *et al.* A TREM2-activating antibody with a blood–brain barrier transport vehicle enhances microglial metabolism in Alzheimer's disease models. *Nat. Neurosci.* **26**, 416–429 (2023).
131. Shuttle Unloads More Gantenerumab into The Brain. *Alzforum* (2021). Available at: https://www.alzforum.org/news/conference-coverage/shuttle-unloads-more-gantenerumab-brain. (Accessed: 30th July 2023)
132. Sehlin, D. *et al.* Antibody-based PET imaging of amyloid beta in mouse models of Alzheimer's disease. *Nat. Commun.* **7**, 1–11 (2016).
133. Sehlin, D., Fang, X. T., Meier, S. R., Jansson, M. & Syvänen, S. Pharmacokinetics, biodistribution and brain retention of a bispecific antibody-based PET radioligand for imaging of amyloid-β. *Sci. Rep.* **7**, 1–9 (2017).
134. Syvänen, S. *et al.* A bispecific Tribody PET radioligand for visualization of amyloid-beta protofibrils – a new concept for neuroimaging. *Neuroimage* **148**, 55–63 (2017).
135. Meier, S. R. *et al.* Antibody-based in vivo PET imaging detects amyloid-ß reduction in Alzheimer transgenic mice after BACE-1 inhibition. *J. Nucl. Med.* **59**, 1885–1891 (2018).
136. Fang, X. T. *et al.* High detection sensitivity with antibody-based PET radioligand for amyloid beta in brain. *Neuroimage* **184**, 881–888 (2019).
137. Syvänen, S. *et al.* Fluorine-18-Labeled Antibody Ligands for PET Imaging of Amyloid-β in Brain. *ACS Chem. Neurosci.* **11**, 4460–4468 (2020).
138. Gustavsson, T., Syvänen, S., O'Callaghan, P. & Sehlin, D. SPECT imaging of distribution and retention of a brain-penetrating bispecific amyloid-β antibody in a mouse model of Alzheimer's disease. *Transl. Neurodegener.* **9**, 1–11 (2020).
139. Meier, S. R. *et al.* 11C-PiB and 124I-Antibody PET Provide Differing Estimates of Brain Amyloid-β after Therapeutic Intervention. *J. Nucl. Med.* **63**, 302–309 (2022).
140. Roshanbin, S. *et al.* Neuropharmacology in vivo imaging of alpha-synuclein with antibody-based PET. *Neuropharmacology* **208**, 1–10 (2022).
141. Schlein, E. *et al.* Functionalization of Radiolabeled Antibodies to Enhance Peripheral Clearance for High Contrast Brain Imaging. *Mol. Pharm.* **19**, 4111–4122 (2022).
142. Wuensche, T. E. *et al.* Advancing 89Zr-immuno-PET in neuroscience with a bispecific anti-amyloid-beta monoclonal antibody – The choice of chelator is essential. *Theranostics* **12**, 7067–7079 (2022).
143. Stergiou, N. *et al.* Application of 89Zr-DFO*-immuno-PET to assess improved target engagement of a bispecific anti-amyloid-ß monoclonal antibody. *Eur. J. Nucl. Med. Mol. Imaging* **50**, 1306–1317 (2023).
144. Faresjö, R. *et al.* Brain pharmacokinetics of two BBB penetrating bispecific antibodies of different size. *Fluids Barriers CNS* **18**, 1–15 (2021).
145. Lopes van den Broek, S. *et al.* Pretargeted Imaging beyond the Blood–Brain Barrier—Utopia or Feasible? *Pharmaceuticals* **15**, 1–15 (2022).
146. Meier, S. R., Sehlin, D., Hultqvist, G. & Syvänen, S. Pinpointing Brain TREM2 Levels in Two Mouse Models of Alzheimer's Disease. *Mol. Imaging Biol.* **23**, 665–675 (2021).

147. Faresjö, R. *et al.* Transferrin Receptor Binding BBB-Shuttle Facilitates Brain Delivery of Anti-Aβ-Affibodies. *Pharm. Res.* **39**, 1509–1521 (2022).
148. Nielsen, S. S. E. *et al.* Apicobasal transferrin receptor localization and trafficking in brain capillary endothelial cells. *Fluids Barriers CNS* **20**, 1–15 (2023).
149. Oostindie, S. C., Lazar, G. A., Schuurman, J. & Parren, P. W. H. I. Avidity in antibody effector functions and biotherapeutic drug design. *Nat. Rev. Drug Discov.* **21**, 715–735 (2022).
150. Couch, J. A. *et al.* Addressing safety liabilities of TfR bispecific antibodies that cross the blood-brain barrier. *Sci. Transl. Med.* **5**, (2013).
151. Bien-Ly, N. *et al.* Transferrin receptor (TfR) trafficking determines brain uptake of TfR antibody affinity variants. *J. Exp. Med.* **211**, 233–244 (2014).
152. Haqqani, A. S. *et al.* Intracellular sorting and transcytosis of the rat transferrin receptor antibody OX26 across the blood-brain barrier in vitro is dependent on its binding affinity. *J. Neurochem.* **146**, 735–752 (2018).
153. Chang, H. Y. *et al.* Brain pharmacokinetics of anti-transferrin receptor antibody affinity variants in rats determined using microdialysis. *MAbs* **13**, 1874121 (2021).
154. Faresjö, R., Sehlin, D. & Syvänen, S. Age, dose, and binding to TfR on blood cells influence brain delivery of a TfR-transported antibody. *Fluids Barriers CNS* **20**, 1–17 (2023).
155. Sade, H. *et al.* A human blood-brain barrier transcytosis assay reveals antibody transcytosis influenced by pH-dependent receptor binding. *PLoS One* **9**, e96340 (2014).
156. Arguello, A. *et al.* Molecular architecture determines brain delivery of a transferrin receptor–targeted lysosomal enzyme. *J. Exp. Med.* **219**, e20211057 (2022).
157. Zhao, P. *et al.* Enhanced anti-angiogenetic effect of transferrin receptor-mediated delivery of VEGF-trap in a glioblastoma mouse model. *MAbs* **14**, e2057269 (2022).
158. Morrison, J. I., Metzendorf, N. G., Rofo, F., Petrovic, A. & Hultqvist, G. A single-chain fragment constant design enables easy production of a monovalent blood–brain barrier transporter and provides an improved brain uptake at elevated doses. *J. Neurochem.* **165**, 413–425 (2023).
159. Lee, H. J., Engelhardt, B., Lesley, J., Bickel, U. & Pardridge, W. M. Targeting rat anti-mouse transferrin receptor monoclonal antibodies through blood-brain barrier in mouse. *J. Pharmacol. Exp. Ther.* **292**, 1048–1052 (2000).
160. Zhang, Y. *et al.* Anti-transferrin receptor antibodies and methods of use. Patent No. US 9,708.406 B2 (2017).
161. Jefferies, W. A. *et al.* Transferrin receptor on endothelium of brain capillaries. *Nature* **312**, 162–163 (1984).
162. Kissel, K. *et al.* Immunohistochemical localization of the murine transferrin receptor (TfR) on blood-tissue barriers using a novel anti-TfR monoclonal antibody. *Histochem. Cell Biol.* **110**, 63–72 (1998).
163. Kerchner, G. A. & Boxer, A. L. Bapineuzumab. *Expert Opin. Biol. Ther.* **10**, 1121–1130 (2010).

164. Arrighi, H. M. *et al.* Amyloid-related imaging abnormalities-haemosiderin (ARIA-H) in patients with Alzheimer's disease treated with bapineuzumab: A historical, prospective secondary analysis. *J. Neurol. Neurosurg. Psychiatry* **87**, 106–112 (2016).
165. Abushouk, A. I. *et al.* Bapineuzumab for mild to moderate Alzheimer's disease: A meta-analysis of randomized controlled trials. *BMC Neurol.* **17**, 1–13 (2017).
166. Cunningham, B. C. & Wells, J. A. High-resolution epitope mapping of hGH-receptor interactions by alanine-scanning mutagenesis. *Science (80-.).* **244**, 1081–1085 (1989).
167. Bonvicini, G. *et al.* ImmunoPET imaging of amyloid-beta in a rat model of Alzheimer's disease with a bispecific, brain-penetrating fusion protein. *Transl. Neurodegener.* **11**, 1–14 (2022).
168. Elliott, J. M. *et al.* Antiparallel conformation of knob and hole aglycosylated half-antibody homodimers is mediated by a CH2-CH3 hydrophobic interaction. *J. Mol. Biol.* **426**, 1947–1957 (2014).
169. Atwell, S., Ridgway, J. B. B., Wells, J. A. & Carter, P. Stable heterodimer from remodeling the domain interface of a homodimer using a phage display library. *J. Mol. Biol.* **270**, 26–35 (1997).
170. Merchant, A. M. *et al.* An efficient route to human bispecific IgG. *Nat. Biotechnol.* **16**, 677–681 (1998).
171. Giese, G., Williams, A., Rodriguez, M. & Persson, J. Bispecific antibody process development: Assembly and purification of knob and hole bispecific antibodies. *Biotechnol. Prog.* **34**, 397–404 (2018).
172. Saunders, K. O. Conceptual approaches to modulating antibody effector functions and circulation half-life. *Front. Immunol.* **10**, 1–20 (2019).
173. Schlothauer, T. *et al.* Novel human IgG1 and IgG4 Fc-engineered antibodies with completely abolished immune effector functions. *Protein Eng. Des. Sel.* **29**, 457–466 (2016).
174. Shields, R. L. *et al.* High Resolution Mapping of the Binding Site on Human IgG1 for FcγRI, FcγRII, FcγRIII, and FcRn and Design of IgG1 Variants with Improved Binding to the FcγR. *J. Biol. Chem.* **276**, 6591–6604 (2001).
175. Lo, M. *et al.* Effector-attenuating substitutions that maintain antibody stability and reduce toxicity in mice. *J. Biol. Chem.* **292**, 3900–3908 (2017).
176. Patching, S. G. Surface plasmon resonance spectroscopy for characterisation of membrane protein-ligand interactions and its potential for drug discovery. *Biochim. Biophys. Acta* **1838**, 43–55 (2014).
177. Hunter, S. A. & Cochran, J. R. Cell-Binding Assays for Determining the Affinity of Protein–Protein Interactions: Technologies and Considerations. in *Methods in Enzymology* **580**, 21–44 (Academic Press Inc., 2016).
178. Cohen, R. M. *et al.* A transgenic alzheimer rat with plaques, tau pathology, behavioral impairment, oligomeric Aβ, and frank neuronal loss. *J. Neurosci.* **33**, 6245–6256 (2013).
179. Chaney, A. M. *et al.* Prodromal neuroinflammatory, cholinergic and metabolite dysfunction detected by PET and MRS in the TgF344-AD transgenic rat model of AD: A collaborative multi-modal study. *Theranostics* **11**, 6644–6667 (2021).

180. Saito, T. *et al.* Single App knock-in mouse models of Alzheimer's disease. *Nat. Neurosci.* **17**, 661–663 (2014).
181. Gustavsson, T. *et al.* Long□term effects of immunotherapy with a brain penetrating Aβ antibody in a mouse model of Alzheimer's disease. *Alzheimers. Res. Ther.* **15**, 1–16 (2023).
182. Triguero, D., Buciak, J. & Pardridge, W. M. Capillary Depletion Method for Quantification of Blood–Brain Barrier Transport of Circulating Peptides and Plasma Proteins. *J. Neurochem.* **54**, 1882–1888 (1990).
183. Zhou, Q. H., Lu, J. Z., Hui, E. K. W., Boado, R. J. & Pardridge, W. M. Delivery of a Peptide Radiopharmaceutical to Brain with an IgG-Avidin Fusion Protein. *Bioconjug. Chem.* **22**, 1611–1618 (2011).
184. Greenwood, F. C., Hunter, W. M. & Glover, J. S. The Preparation of I-131-Labelled Human Growth Hormone of High Specific. *Biochem. J.* **89**, 114–123 (1963).
185. Conti, M. & Eriksson, L. Physics of pure and non-pure positron emitters for PET: A review and a discussion. *EJNMMI Phys.* **3**, 1–17 (2016).
186. Bailey, D. L., Humm, J. L., Todd-Pokropek, A. & van Aswegen, A. *Nuclear Medicine Physics: A Handbook for Teachers and Students*. *International Atomic Energy Agency* (2014).
187. Solon, E. G., Schweitzer, A., Stoeckli, M. & Prideaux, B. Autoradiography, MALDI-MS, and SIMS-MS imaging in pharmaceutical discovery and development. *AAPS J.* **12**, 11–26 (2010).
188. Boado, R. J., Zhang, Y., Wang, Y. & Pardridge, W. M. Engineering and expression of a chimeric transferrin receptor monoclonal antibody for blood-brain barrier delivery in the mouse. *Biotechnol. Bioeng.* **102**, 1251–1258 (2009).
189. Stocki, P. *et al.* Blood-brain barrier transport using a high affinity, brain-selective VNAR antibody targeting transferrin receptor 1. *FASEB J.* **35**, 1–19 (2021).
190. Gustafsson, S. *et al.* Blood-brain barrier integrity in a mouse model of Alzheimer's disease with or without acute 3D6 immunotherapy. *Neuropharmacology* **143**, 1–9 (2018).
191. Repetto-Llamazares, A., Abbas, N., Bruland, Ø. S., Dahle, J. & Larsen, R. H. Advantage of Lutetium-177 versus Radioiodine Immunoconjugate in Targeted Radionuclide Therapy of B-cell Tumors. *Anticancer Res.* **34**, 3263–3270 (2014).
192. Cohen-Dvashi, H. *et al.* Rational design of universal immunotherapy for TfR1-tropic arenaviruses. *Nat. Commun.* **11**, 1–11 (2020).
193. Sjöström, D. J., Berger, S. A., Oberdorfer, G. & Bjelic, S. Computational backbone design enables soluble engineering of transferrin receptor apical domain. *Proteins Struct. Funct. Bioinforma.* **88**, 1569–1577 (2020).

Acta Universitatis Upsaliensis

Digital Comprehensive Summaries of Uppsala Dissertations from the Faculty of Medicine 1962

Editor: The Dean of the Faculty of Medicine

A doctoral dissertation from the Faculty of Medicine, Uppsala University, is usually a summary of a number of papers. A few copies of the complete dissertation are kept at major Swedish research libraries, while the summary alone is distributed internationally through the series Digital Comprehensive Summaries of Uppsala Dissertations from the Faculty of Medicine. (Prior to January, 2005, the series was published under the title "Comprehensive Summaries of Uppsala Dissertations from the Faculty of Medicine".)

Distribution: publications.uu.se
urn:nbn:se:uu:diva-507816

ACTA UNIVERSITATIS
UPSALIENSIS
2023